

**Development and Analysis of Computationally Efficient
Methods for Analyzing Surface Effects**

**A DISSERTATION
SUBMITTED TO THE FACULTY OF THE GRADUATE SCHOOL
OF THE UNIVERSITY OF MINNESOTA
BY**

Andrew J. Binder

**IN PARTIAL FULFILLMENT OF THE REQUIREMENTS
FOR THE DEGREE OF
Doctor of Philosophy**

Mitchell Luskin

January, 2017

© Andrew J. Binder 2017
ALL RIGHTS RESERVED

Acknowledgements

It has been my pleasure over my graduate career to have the opportunity to work with many great people. I would like to first thank my advisor Mitchell Luskin for his patience and support. It has been a privilege working with him.

I would also like to extend my deepest thanks to Christoph Ortner, who was a collaborator on much of the work presented in this thesis. I have learned a tremendous amount of mathematics from him and thank him for hosting me for a semester at the University of Warwick.

I thank Danny Perez and Art Voter for having me as a summer intern at Los Alamos National Laboratory. I learned much in our work together and thoroughly enjoyed the experience. Our work there has been published in [1], but a discussion of this material is not included in the thesis.

I would also like to thank Gideon Simpson and Tony Lelièvre for their early collaboration with me. Our work was published in [2]. In particular, I would like thank Gideon for the advice and guidance he provided to me during his time at the University of Minnesota. I would also like to thank David Aristoff for his helpful comments during this project.

I would like to thank the many excellent professors and staff at the University of Minnesota. My knowledge of mathematics has grown considerably during my time here. I would like to thank Bonny Flemming in particular for her great help in answering any and all questions I have had over the years. She has always been a wonderful help and exceedingly patient. Finally, I would like to acknowledge my many friends and colleagues that I have had the pleasure of meeting with over my time at the U that has made my stay so enjoyable.

Material from Chapters 2 and 4 has been submitted for publication in [3].

Dedication

To my loving family, thank you for your support.

Abstract

Experiments have shown that materials at the nanoscale exhibit new material properties compared to their macro-counterparts as a result of surface effects. We rigorously examine an atomistic model that exhibits surface effects and estimate the rate of decay of this influence. Despite the highly localized nature of surface effects, the regular Cauchy-Born method is shown to be incapable of capturing the surface physics in these systems. Two methods that seek to accurately model the influence of surfaces in a molecular statics problem are examined.

First, the surface Cauchy-Born method is examined. An asymptotic analysis is performed to investigate the behavior of this method, and it is shown that the method does represent an improvement over the regular Cauchy-Born method. However, it does not fully capture the surface behavior. Next, a novel predictor-corrector method is introduced to better capture these effects. Using the regular Cauchy-Born solution as a predictor for material behavior, the solution is corrected over a small boundary layer at the surface of a 1D material. The decomposition of the approximation into a bulk and surface component is justified in the analysis, and the convergence of the approximation to the atomistic solution is shown. The analysis for both methods is then verified numerically.

Contents

Acknowledgements	i
Dedication	ii
Abstract	iii
List of Figures	vi
1 Introduction	1
2 Atomistic and Cauchy–Born Models	5
2.1 Atomistic Model	5
2.1.1 Surface Problem	9
2.1.2 Existence and Stability of Atomistic Solutions	12
2.2 Cauchy–Born Model	21
2.2.1 Inconsistency of Cauchy–Born Method	21
2.2.2 Existence and Regularity of Cauchy–Born Solutions	23
3 Surface Cauchy–Born Method	29
3.1 Analysis of the Linearized Systems	32
3.1.1 Projected 3D Model	36
3.2 Asymptotic Analysis	38
3.2.1 Strain Relative Error Analysis	39
4 Predictor-Corrector Method	44
4.1 Corrector Model	44

4.2	Predictor-Corrector Approximation	51
4.2.1	Error Bound in Terms of the External Forces	59
4.3	Numerical Results	61
5	Conclusion	67
	References	69
	Appendix A. Common Results	74
A.1	Variations in Energies	74
A.2	Inverse Function Theorem	75

List of Figures

2.1	Illustration of interactions at surface and interior of model.	7
3.1	Computed ground states according to the linearized atomistic and the discretized surface Cauchy–Born method for two different surface element sizes.	36
3.2	Visualization of the projection of $(0, 0, 1)$ planes of atoms into a 1D chain of atoms.	37
3.3	ℓ_2 Pointwise and Mean Relative Error Decay Rates	43
4.1	Ground states for the atomistic and Cauchy–Born models.	62
4.2	Ground states for the atomistic model and the predictor-corrector method.	63
4.3	Rate of convergence to atomistic solution in infinite boundary layer limit.	64
4.4	Rate of convergence to atomistic solution in the long-wavelength limit.	65
4.5	Energy-minimizing configuration for atomistic and predictor-corrector systems in the presence of external forces ($L = 5$).	65
4.6	Demonstration of non-vanishing error in the presence of non-zero external forces and increasing boundary layer.	66

Chapter 1

Introduction

Nano-structures and materials such as carbon nanotubes, nanowires, and quantum dots have become an increasingly important field of study due to the growing importance of nanotechnology. The study of nanostructures has drawn special interest due to the fact that they often exhibit properties incongruent with their macro-counterparts. This size-dependence in material properties is attributed to the greater influence of surface effects at smaller length scales [4-6]. Near the surface, atoms experience a different bonding environment as compared to atoms in an idealized crystalline material. This results in surface elastic behavior differing from that of the interior. For smaller materials, where the surface area to volume ratio becomes large, surface effects eventually come to play a greater role in the material behavior. Size-dependent material properties driven by the predominance of these surface effects that have been experimentally observed include new phase transformations [7], shape memory behavior [8], and yield strengths in nanowires an order of magnitude greater than the wires' bulk counterparts [9]. Additionally, even in bulk crystals, when the region of interest lies at or near the crystal boundary, accurately capturing surface physical remains crucial. In experiments such as nano-indentation [10,11], surface effects can play a tremendous role despite having negligible effect on the system as a whole.

Computational models that can take into account surface effects are an important avenue of research in the study and understanding of these phenomena. Despite the “small” size of these systems, fully atomistic simulations are often prohibitively expensive due to the number of degrees of freedom in the system. In order to reduce

computational cost, it is common to use a classical atomistic description of the system with the interaction amongst the constituents of the model governed by an empirical potential as opposed to the far more expensive density functional theory (DFT) or tight-binding approaches [12]. Even with the utilization of this classical model, though, a computationally efficient approach is desirable and often still necessary to study these systems numerically. In this paper, we consider and develop alternative computationally efficient approaches to simulating surface systems.

For larger or bulk systems absent of defects, continuum elasticity models have often served as efficient and reliable methods to study material properties. The Cauchy–Born method [12, 13] is one example of such a model that is useful for approximating macro-scale materials. In the Cauchy–Born approach, the non-local interactions of the atomistic system are replaced by a localized continuum approximation. This is accomplished through a limiting process of the atomistic model so that the underlying lattice structure and potential in the atomistic system inform the continuum model [13–16]. This continuum model may then be further approximated using the finite-element method (FEM), which allows for a further reduction in the number of degrees of freedom in the system. This leads to a much reduced computational cost for simulation. However, this approach fails in the presence of defects since they create rapid variations in the atomistic displacement field which cannot be accurately captured by the Cauchy–Born model. In particular for this work, the Cauchy–Born method struggles with the inclusion of surfaces [17–19]. When the aforementioned limiting procedure is applied to produce the Cauchy–Born model, only a uniform volumetric energy density remains. The surface behavior is lost in the process.

Despite the failure of the Cauchy–Born method in capturing surface effects, it is still quite efficient at capturing bulk material behavior. For this reason, many approaches to efficient computational schemes for studying material behavior include the Cauchy–Born method in some form or another. In the quasicontinuum methods, a combination of the atomistic and continuum models are used to describe the system [20–24]. The atomistic model is used in regions containing defects, in this case at the surface, while the remainder of the system is treated with the continuum model. Typically, the atomistic region is quite localized so that usage of the Cauchy–Born model outside of this region can lead to large computational savings. Great care must, of course, be taken

at the interface or “handshake” region where the two models are coupled. The coupling region can introduce an additional source of error into the approximation and understanding this region’s impact is central to guaranteeing the fidelity of the entire method of approximation. In energy-based quasicontinuum methods, spurious forces known as ghost forces are often introduced due the coupling mechanism [25, 26]. In force-based quasicontinuum methods, energy conservation is lost as a result of this coupling [25, 27, 28]. Addressing and understanding the consequences of the various coupling mechanisms is a major area of research in the field of quasicontinuum methods. Research in this area has led to new blended quasicontinuum methods [29–31] and optimization based atomistic-to-continuum coupling approaches [32]. Other methods that have been proposed to efficiently capture surface physics generally entail a modification of the continuum model [33–36].

While the aforementioned methods do result in a superior approximation than that which comes from the regular Cauchy–Born method, they still have notable drawbacks for studying surface-dominated systems. The modified continuum models lack a systematic control over the error in their approximation. In addition, computing the additional surface elasticity constants for the new surface stress tensor requires its own set of computations that are often quite expensive. The various atomistic-to-continuum coupling methods may suffer from the fact that surfaces are not quite as localized as the defects it is generally meant to examine, increasing computational cost. Certain surface geometries such as nanowires may be especially troublesome for the approach and significantly diminish any potential computational savings.

In this work, we discuss two approaches to considering surface physics in the case of the classical atomistic description. First, we discuss the surface Cauchy–Born method as introduced by Harold Park et al [17–19, 19, 37, 38]. The surface Cauchy–Born method attempts to restore a key property of the Cauchy–Born method that is lost when surfaces are introduced into the system. Namely, the surface Cauchy–Born method seeks to introduce a surface energy integral so that the surface Cauchy–Born and atomistic energies and forces agree in the case of a homogeneous strain. This surface energy integral is found in a limiting process of the surface energy terms analogously to the bulk case so that the integral depends on the surface structure and potential. An energy variational formulation consisting of these surface and bulk contributions may then be

solved using standard non-linear finite element techniques to determine the material response. The surface Cauchy–Born method has already been applied to a variety of problems in the literature.

After discussing this model, we introduce a novel approach to efficiently and accurately capturing surface behavior through the use of a predictor-corrector method. In this predictor-corrector method, the Cauchy–Born method serves as the initial predictor for material behavior. As the Cauchy–Born method works well for studying macro-materials, it should serve as an excellent approximation for the response of the material away from the surface. Since the usual Cauchy–Born method is used, the standard techniques may be used to efficiently solve this problem. The solution for the Cauchy–Born method is then corrected over a boundary layer near the surface to capture surface effects. The size of the boundary layer is a controllable parameter in this predictor-corrector method and allows for a systematic control over the accuracy of the approximation. Proving the validity of the decomposition of the atomistic solution into a bulk response and surface correction will be the primary goal of the analysis for this method in addition to assessing the quality of the approximation.

We start the analysis with the formulation of the atomistic model that we will consider throughout. We rigorously analyze the model and examine the rate of decay of surface effects. In the next chapters, we analyze the surface Cauchy–Born and predictor-corrector methods discussed above.

Chapter 2

Atomistic and Cauchy–Born Models

2.1 Atomistic Model

As stated in the introduction, the primary model which we will be examining in this work will be a semi-infinite, 1D chain of atoms. This model will contain only one ‘surface’: the endpoint of the chain. This is the simplest setting in which we can still observe non-trivial surface effects.

We index the atoms in the chain by the set of non-negative integers or $\mathbb{Z}_{\geq 0}$, and we denote the individual location of the atom with index ℓ in the chain by $y_\ell \in \mathbb{R}$. The reference position of each atom in the chain is chosen to be $y_\ell = \ell$ for all $\ell \in \mathbb{Z}_{\geq 0}$ with the unit for distance taken to be the equilibrium spacing for the corresponding infinite chain model to be described later. We denote the displacement of atom ℓ from its reference position with $u_\ell \in \mathbb{R}$; that is, $u_\ell := y_\ell - \ell$. The displacement gradient, or the strain in the nearest-neighbor bond between the atoms indexed by ℓ and $\ell + 1$ in the chain, will be written as

$$u'_\ell := u_{\ell+1} - u_\ell = y_{\ell+1} - y_\ell - 1. \quad (2.1)$$

Physically, the strain u'_ℓ indicates the change in distance between two adjacent atoms with indices ℓ and $\ell + 1$ from their reference bond length. Under this choice of reference

lattice, the surface will be located at the atom with index 0 in the reference configuration.

The atoms in this semi-infinite chain will interact according to a nearest-neighbor, many-body model. Such a model permits both nearest-neighbor, many-body interactions and next-nearest neighbor interactions. We define the energy for this system to be

$$\mathcal{E}^a(y) := V^{\text{surf}}(y_1 - y_0) + \sum_{\ell=1}^{\infty} V(y_\ell - y_{\ell-1}, y_{\ell+1} - y_\ell),$$

where V denotes the site energy for atoms in the interior of the system while V^{surf} denotes the surface site energy.

Site energies indicate the energy contribution that can be assigned to an individual atom as a result of its interactions with the rest of the system and are useful for simply distinguishing between generalized surface and bulk components of the chain in the analysis. The surface bond merits a different site energy than the interior atoms because the 0-th atom has only one nearest neighbor while every other atom in the interior has two. The surface site energy, however, is related to the bulk energy in that it will be assumed to be the limit of the bulk site energy as one of the bonds is stretched to infinity.

We observe that the energy \mathcal{E}^a is translation invariant due to the fact that the energy depends only on bond lengths and note that we do not consider configurations that differ only by a translation to be meaningfully different. As such, we consider only equivalence classes of the set of all permissible configurations formed by equating configurations that differ only by a uniform translation of the chain's elements. In the analysis, we will consider only the representative configurations with the end point at zero, or $y_0 = 0$. Fixing the endpoint has the added effect of making knowledge of the strain in the entire chain, or knowledge of u' , equivalent to knowing the deformation of the chain, which we denoted by y . With this equivalency, it will often be more convenient to consider the energy in terms of the strain rather than the deformation since this reduces the number of independent arguments in each site energy. In terms of the strain, the total energy is

$$\mathcal{E}^a(u) := V^{\text{surf}}(1 + u'_0) + \sum_{\ell=1}^{\infty} V(1 + u'_{\ell-1}, 1 + u'_\ell).$$

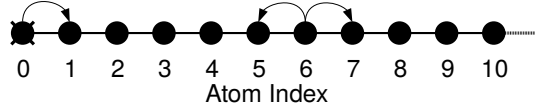


Figure 2.1: Illustration of interactions at surface and interior of model.

For notational convenience, we absorb the 1 into the site energy functions so that we may write $V(u'_{\ell-1}, u'_\ell) := V(1 + u'_{\ell-1}, 1 + u'_\ell)$ and $V^{\text{surf}}(u'_0) := V^{\text{surf}}(1 + u'_0)$. Finally, we arrive at the energy equation that we shall use most often throughout this work:

$$\mathcal{E}^a(u) := V^{\text{surf}}(u'_0) + \sum_{\ell=1}^{\infty} V(u'_{\ell-1}, u'_\ell), \quad (2.2)$$

An illustration of the model under consideration is provided in Fig. 2.1

The site energies V and V^{surf} shall be assumed to satisfy the following properties:

Site Energy Properties:

- (i) $V \in C^k(\mathbb{R}^2)$ and $V^{\text{surf}} \in C^k(\mathbb{R})$ with $k \geq 3$;
- (ii) V, V^{surf} and all permissible partial derivatives are bounded.
- (iii) $V(0, 0) = 0$;
- (iv) $\partial^2 V(0, 0) > 0$;
- (v) $\inf_{\{|(r,s)|>\varepsilon\}} V(r, s) > 0$ for any $\varepsilon > 0$;
- (vi) For any $s \in \mathbb{R}$, $\lim_{r \rightarrow \infty} V(r, s) = V^{\text{surf}}(s)$;

Properties (iii)–(v) together may be used to deduce the exact ground state of the infinite bulk model of our system without surfaces. In this bulk model, the energy is given by

$$\mathcal{E}^{\infty\text{-chain}} := \sum_{\ell=-\infty}^{\infty} V(u'_{\ell-1}, u'_\ell)$$

and the energy-minimizing configuration would be given by $y_\ell = \ell$ for all $\ell \in \mathbb{Z}$. Assuming the reference configuration was given by $y_\ell = \ell$ as well, this would correspond to a uniform strain of zero. Property (iv) guarantees the stability of the ground state for

this infinite chain system. In contrast, these properties for the site energies do not yield an explicit solution for the ground state of the semi-infinite chain system. They are enough, however, to prove the existence of a ground state for the surface system as well as provide information on the effective region over which surface effects are relevant, which will be of importance in developing a method to effectively model these effects below in this work.

An important consequence of these site energy properties concerns the infimum of V^{surf} . The surface site energy is defined in terms of the limiting behavior of the bulk site energy by property (vi). Combining this fact with properties (v) and (vi), we see that

$$\inf_{s \in \mathbb{R}} V^{\text{surf}}(s) > 0. \quad (2.3)$$

Essentially, this property states that surfaces cost energy for the system to form. This is to be expected as, if this were not the case, the system would immediately fracture and split apart. While this result should therefore be considered physically obvious, it will play an important role in the proof of the existence of a ground state for the surface problem.

Property (ii) is one of convenience and is not strictly necessary. The results in this work hold without this assumption, but it is standard in the field to include it. To see how this assumption may be removed, see e.g. [39].

To conclude the discussion of the consequences and implications of the site energy assumptions, we remark that properties (i) and (ii) ensure that the first and second variations of the total energy are globally Lipschitz continuous. We refer to [24] for this simple proof.

We denote derivatives of V^{surf} with respect to its argument by $\partial_F V^{\text{surf}}$. Derivatives of V with respect to its first and second argument will be denoted by $\partial_1 V$ and $\partial_2 V$, respectively. Higher-order derivatives for the two site energies will be denoted similarly. For example, $\partial_{12} V$ denotes the derivative of V with respect to its first and second arguments.

2.1.1 Surface Problem

For the generalized semi-infinite model, we are concerned with finding the energy-minimizing configuration of the chain in the presence of external forces. Such a problem requires that we define the space of allowable configurations of the chain as well as what constitutes an acceptable external force. For the former, we restrict our attention to the configurations admissible in the following finite-energy space of displacements:

$$\mathcal{U} := \{u : \mathbb{Z}_{\geq 0} \rightarrow \mathbb{R} \mid u(0) = 0 \text{ and } u' \in \ell^2(\mathbb{Z}_{\geq 0})\}. \quad (2.4)$$

The fixation of the surface necessitates that $u(0) = 0$. With this imposition, the seminorm $|u| := \|u'\|_{\ell^2(\mathbb{Z}_{\geq 0})}$ becomes a norm. The space \mathcal{U} becomes a Hilbert space when equipped with this norm. It is easy to see (e.g., as shown in [24]) that compact displacements are dense in \mathcal{U} so that, for arbitrary elements of \mathcal{U} , we may define the energy \mathcal{E}^a by continuity. In this analysis, we consider only externally applied forces which are elements of \mathcal{U}^* and take the form of a lattice function $f : \mathbb{Z}_{\geq 0} \rightarrow \mathbb{R}$. These applied forces represent dead-load forces, which are permanently-applied, static forces. We say that $f \in \mathcal{U}^*$ if and only if there exists a constant $\|f\|_{\mathcal{U}^*}$ such that

$$|\langle f, u \rangle| \leq \|f\|_{\mathcal{U}^*} \|u'\|_{\ell^2(\mathbb{Z}_{\geq 0})} \quad \text{for all } u \in \mathcal{U} \text{ with } \text{supp}(u) \text{ compact,}$$

where $\langle f, u \rangle := \sum_{\ell=0}^{\infty} f_{\ell} u_{\ell}$. For arbitrary $u \in \mathcal{U}$, $\langle f, u \rangle$ is defined by continuity using compact displacements as usual.

With the space \mathcal{U} and the external forces defined, we may now state the atomistic surface problem. Given a force $f \in \mathcal{U}^*$, we seek a minimizer

$$u^a \in \arg \min \{ \mathcal{E}^a(u) - \langle f, u \rangle_{\mathbb{Z}_{\geq 0}} \mid u \in \mathcal{U} \}. \quad (2.5)$$

This problem may have a unique solution, several solutions, or no solutions. The existence and regularity of these solutions is studied in the next section.

Remark. It is possible to rewrite the inner product $\langle f, u \rangle$ into another inner product in terms of the strain u' . To do so, we first observe that $f \in \mathcal{U}^*$ if and only if there exists a $g \in \ell^2(\mathbb{Z}_{\geq 0})$ such that $f = -g'$, where we define g' here according to $g'_{\ell} = g_{\ell} - g_{\ell-1}$

and use the convention that $g_{-1} = 0$. This can be proven by considering a discrete summation by parts of $\langle f, u \rangle$ and by using the Riesz representation theorem from [40]. Using this approach, it can also be shown that

$$g_n = \sum_{\ell=n+1}^{\infty} f_{\ell} < \infty.$$

Below, in lemma 2.2.2, we show that this sum is well-defined. Therefore, $\langle f, u \rangle = \langle g, u' \rangle \leq \|g\|_{\ell^2} \|u'\|_{\ell^2}$. An easy consequence of this fact is that $\|f\|_{\mathcal{U}^*} = \|g\|_{\ell^2}$.

Example: Embedded-Atom Model

In these example sections, we discuss two concrete examples of systems that are encompassed by our general model described above. First, we show that a nearest-neighbor Embedded Atom Model (EAM) [41, 42] with only nearest-neighbor interactions for the semi-infinite chain system is contained in this framework. We may write the energy for such a system in terms of the strain in the following way:

$$\mathcal{E}^a(u') = \phi(1 + u'_0) + \psi(\rho(1 + u'_0)) + \sum_{\ell=1}^{\infty} \left[\phi(1 + u'_\ell) + \psi(\rho(1 + u'_\ell) + \rho(1 + u'_{\ell-1})) \right], \quad (2.6)$$

where ϕ is a nearest-neighbor pair potential, ψ is an embedding energy function, and ρ is an electron density function. The electron density function ρ describes the electron density contribution from a single atom as a function of the distance away from the atom. The embedding energy function ψ represents the energy required to place an atom in a location with the given electronic density. By defining the bulk and site energies, respectively, as

$$V(u'_{\ell-1}, u'_\ell) = \frac{1}{2}\phi(1 + u'_{\ell-1}) + \frac{1}{2}\phi(1 + u'_\ell) + \psi(\rho(1 + u'_{\ell-1}) + \rho(1 + u'_\ell)), \quad \text{and} \\ V^{\text{surf}}(u'_0) = \frac{1}{2}\phi(1 + u'_0) + \psi(\rho(1 + u'_0)),$$

we see that the generalized energy equation in Eq. (2.2) becomes the EAM energy defined above.

In the analysis portion of this work, our focus will remain on the generalized form of the energy. However, we will return to the EAM model specifically for numerical experiments throughout the paper. Specifically, for the atomistic model, we will use the EAM site energies described in (2.6) with ϕ , ψ , and ρ given by

$$\begin{aligned}\phi(r) &= \phi_e \exp\left(-\gamma\left(\frac{r}{r_e} - 1\right)\right), & \rho(r) &= f_e \exp\left(-\beta\left(\frac{r}{r_e} - 1\right)\right), \\ \psi(\rho) &= -E_c \left[1 - \frac{\alpha}{\beta} \log\left(\frac{\rho}{\rho_e}\right)\right] \left(\frac{\rho}{\rho_e}\right)^{\alpha/\beta} - \phi_e \left(\frac{\rho}{\rho_e}\right)^{\gamma/\beta},\end{aligned}$$

where $\phi_e = 10.6$, $f_e = 1$, $E_c = 3.54$, $\alpha = 21$, $\beta = 6$, $\rho_e = 2$, $r_e = 1$, and $\gamma = 8$. These parameters and potentials are taken from [41] and represent an EAM potential describing a system composed of copper atoms. We note that r_e represents the equilibrium distance in the infinite atomistic model without surfaces. Therefore, the equilibrium spacing in the infinite model is simply 1 and corresponds to a strain of 0 as our reference spacing is also 1. We also note that property (ii) of the site energies does not hold for this choice of energy, but as mentioned in the earlier discussion of the site energy assumptions, the results for the predictor-corrector method are unchanged with this assumption removed.

Example: Next-Nearest Neighbor Model

We next consider a next-nearest neighbor type model and show again how the bulk and surface site energies must be defined in this framework. Consider the following next-nearest neighbor system energy for the semi-infinite chain:

$$\mathcal{E}^a(u') = \phi(1 + u'_0) + \sum_{\ell=1}^{\infty} \left[\phi(1 + u'_\ell) + \phi(2 + u'_{\ell-1} + u'_\ell) \right],$$

where ϕ is some potential such as a Lennard-Jones potential [43, 44]. To translate this into the form of (2.2), we define the bulk and surface site energies, respectively, as

$$\begin{aligned}V(u'_{\ell-1}, u'_\ell) &= \frac{1}{2}\phi(1 + u'_{\ell-1}) + \frac{1}{2}\phi(1 + u'_\ell) + \phi(2 + u'_{\ell-1} + u'_\ell) \quad \text{and} \\ V^{\text{surf}}(u'_0) &= \frac{1}{2}\phi(1 + u'_0).\end{aligned}$$

2.1.2 Existence and Stability of Atomistic Solutions

Unlike for the infinite atomistic model without surfaces that was briefly mentioned above, we do not expect in general that an energy-minimizing configuration for the semi-infinite chain will be one with a homogeneous strain. Instead, we expect that a minimizer will exhibit some form of surface effects. As such, we do not expect to be able to derive an explicit solution for our atomistic problem. We must be satisfied with weaker results. In this section, we prove the existence of minimizers to the atomistic problem, consider the stability of such solutions, and examine their decay rates.

Theorem 2.1.1. *There exists a minimizer of $\mathcal{E}^a : \mathcal{U} \rightarrow \mathbb{R} \cup \{+\infty\}$.*

Proof. The proof for the existence of the minimizer will closely follow the direct method from the calculus of variations. To begin with, we establish that the infimum of the atomistic energy is finite and that the atomistic energy functional is bounded below. Property (iii) on the site potential energies and the fact that $|V^{\text{surf}}(0)| < \infty$ together imply that $\mathcal{E}^a(0) < \infty$. Property (v) and Eq. (2.3) show that the atomistic energy is bounded below by 0. Thus, we have that

$$0 \leq \inf_{u \in \mathcal{U}} \mathcal{E}^a(u) < \infty.$$

We may then consider an energy minimizing sequence $\{u_n\}_{n=1}^\infty \subset \mathcal{U}$ such that

$$\mathcal{E}^a(u_n) \rightarrow \inf_{u \in \mathcal{U}} \mathcal{E}^a(u) \quad \text{and} \quad \mathcal{E}^a(u_n) < \inf_{u \in \mathcal{U}} \mathcal{E}^a(u) + 1, \quad (2.7)$$

where the latter condition was added without loss of generality.

We now wish to show that the norm $\|u'_n\|_{\ell^2(\mathbb{Z}_{\geq 0})}$ is uniformly bounded in n ; that is, we will show that there exists some constant $C_{\text{unif}} > 0$ such that $\|u'_n\|_{\ell^2} \leq C_{\text{unif}}$ for all n . To that end, we will separately consider the small and large strain contributions to this norm. Let $\varepsilon > 0$. For each $n \in \mathbb{N}$, we denote the set of indices that indicate the locations of strains larger than ε in the chain to be D_ε^n :

$$D_\varepsilon^n := \{\ell \in \mathbb{Z}_{\geq 0} \mid |u'_{n,\ell}| > \varepsilon\}.$$

The cardinality of D_ε^n is finite for all n since $u_n \notin \mathcal{U}$ otherwise. From the non-negativity

of the site energies, we see that

$$\mathcal{E}^a(u_n) \geq \sum_{\ell \in D_\varepsilon^n} V(u'_\ell, u'_{\ell+1}) \geq \#D_\varepsilon^n \cdot \inf_{|(r', s')| > \varepsilon} V(r', s') \quad (2.8)$$

Property (v) states that the infimum of the bulk site energy is positive. Therefore, the cardinality of D_ε^n must be uniformly bounded; otherwise, there would exist a subsequence of the $\{u_n\}$ would tend to infinite energy contradicting the fact that the $\{u_n\}$ are an energy-minimizing sequence. Thus,

$$\max_n \#D_\varepsilon^n < \infty. \quad (2.9)$$

We now consider the case for small strains. By Taylor's Theorem and Property (iv), we may show that, for small enough ε , there exists a constant $C_\varepsilon > 0$ such that

$$V(u'_{n,\ell}, u'_{n,\ell+1}) \geq C_\varepsilon (|u'_{n,\ell}|^2 + |u'_{n,\ell+1}|^2) \quad \text{for all } \ell \notin D_\varepsilon^n.$$

With this inequality and the non-negativity of the site energies, we obtain

$$\begin{aligned} \mathcal{E}^a(u_n) &= V^{\text{surf}}(u'_{n,0}) + \sum_{\ell \in \mathbb{Z}_{\geq 0}} V(u'_{n,\ell}, u'_{n,\ell+1}) \\ &= V^{\text{surf}}(u'_{n,0}) + \sum_{\ell \in D_\varepsilon^n} V(u'_{n,\ell}, u'_{n,\ell+1}) + \sum_{\ell \notin D_\varepsilon^n} V(u'_{n,\ell}, u'_{n,\ell+1}) \\ &\geq C_\varepsilon \sum_{\ell \notin D_\varepsilon^n} (|u'_{n,\ell}|^2 + |u'_{n,\ell+1}|^2) \geq C_\varepsilon \sum_{\ell \notin D_\varepsilon^n} |u'_{n,\ell}|^2. \end{aligned}$$

Using the bound on the energy from Eq. (2.7), we may show that

$$\sum_{\ell \notin D_\varepsilon^n} |u'_{n,\ell}|^2 \leq C_\varepsilon^{-1} \left(\inf_{u \in \mathcal{U}} \mathcal{E}^a(u) + 1 \right) < \infty. \quad (2.10)$$

Note that the upper bound here is independent of n and that the sum on the left excludes only a finite number of strains on the chain; namely, it excludes the contributions from the strains with ε -defects. If we can show that there exists a positive constant $C > 0$ such that

$$|u'_{n,\ell}| \leq C \quad \text{for all } n \in \mathbb{N}, \quad \ell \in \mathbb{Z}_{\geq 0}, \quad (2.11)$$

then we obtain a uniform bound on $\|u'_n\|_{\ell^2}$ as desired.

Suppose, for contradiction, that (2.11) fails. Then, there exists a subsequence $\{u_{n_k}\}_{k=1}^{\infty}$ and a sequence of indices $\{\ell_k\}_{k=1}^{\infty}$ such that

$$\lim_{k \rightarrow \infty} |u'_{n_k, \ell_k}| \rightarrow \infty. \quad (2.12)$$

Since $\max_n \#D_\varepsilon^n$ is finite, we may add the condition on the indices ℓ_k that there exists a constant $S > 0$ such that

$$|u'_{n_k, \ell_k+1}| \leq S \quad \text{for all } k. \quad (2.13)$$

We now split the chain into two components:

$$\begin{aligned} \mathcal{E}^a(u_{n_k}) &= V^{\text{surf}}(u'_{n_k, 0}) + \sum_{\ell=0}^{\ell_k-1} V(u'_{n_k, \ell}, u'_{n_k, \ell+1}) \\ &\quad + V(u'_{n_k, \ell_k}, u'_{n_k, \ell_k+1}) + \sum_{\ell=\ell_k+1}^{\infty} V(u'_{n_k, \ell}, u'_{n_k, \ell+1}) \\ &=: E_1 + E_2, \end{aligned}$$

where

$$E_1 := V^{\text{surf}}(u'_{n_k, 0}) + \sum_{\ell=0}^{\ell_k-1} V(u'_{n_k, \ell}, u'_{n_k, \ell+1})$$

and

$$E_2 := V(u'_{n_k, \ell_k}, u'_{n_k, \ell_k+1}) + \sum_{\ell=\ell_k+1}^{\infty} V(u'_{n_k, \ell}, u'_{n_k, \ell+1}).$$

Since the V are non-negative, we obtain for E_1 that

$$E_1 = V^{\text{surf}}(u'_{n_k, 0}) + \sum_{\ell=0}^{\ell_k-1} V(u'_{n_k, \ell}, u'_{n_k, \ell+1}) \geq \inf_{s' \in \mathbb{R}} V^{\text{surf}}(s') > 0.$$

To bound E_2 , we observe that the increasing strain at ℓ_k represents a fracture of the chain and the formation of a new surface. Up to a small error, the atoms with index greater than or equal to ℓ_k represent another semi-infinite chain system with a surface, and as such, will have a similar energy contribution. The fracturing of the chain, then,

will inevitably raise the energy of the system and will not approximate an energy-minimizing configuration, leading to a contradiction. To make this precise, let $\varepsilon_1 := \frac{1}{2} \inf_{s \in \mathbb{R}} V^{\text{surf}}(s) > 0$. By properties (i) and (vi), there exists $R > 0$ such that if $|r| > R$, then $|V(r, s) - V^{\text{surf}}(s)| < \varepsilon_1$ for all $|s| \leq S$. From (2.12), there exists a $K > 0$ such that $|u'_{n_k, \ell_k}| > R$ for all $k \geq K$. Therefore, we can conclude that, for $k \geq K$,

$$\begin{aligned} E_2 &= V(u'_{n_k, \ell_k}, u'_{n_k, \ell_k+1}) + \sum_{\ell=\ell_k+1}^{\infty} V(u'_{n_k, \ell}, u'_{n_k, \ell+1}) \\ &\geq V^{\text{surf}}(u'_{n_k, \ell_k+1}) - \varepsilon_1 + \sum_{\ell=\ell_k+1}^{\infty} V(u'_{n_k, \ell}, u'_{n_k, \ell+1}) \\ &\geq \inf_{u \in \mathcal{U}} \mathcal{E}^a(u) - \varepsilon_1. \end{aligned}$$

This inequality together with the previous inequality that contains the energy contribution from the original surface shows that

$$\mathcal{E}^a(u_{n_k}) = E_1 + E_2 \geq \frac{1}{2} \inf_{s \in \mathbb{R}} V^{\text{surf}}(s) + \inf_{u \in \mathcal{U}} \mathcal{E}^a(u)$$

for all $k \geq K$. Since $\frac{1}{2} \inf_{s \in \mathbb{R}} V^{\text{surf}}(s) > 0$, this contradicts the fact that $\{u_{n_k}\}$ is a subsequence of the energy-minimizing configuration sequence. Therefore, we must have that there exists a constant $C > 0$ such that $|u'_{n, \ell}| \leq C$ for all $n \in \mathbb{N}$ and $\ell \in \mathbb{Z}_{\geq 0}$. With Eq. (2.10), it may finally be shown that

$$\|u'_n\|_{\ell^2(\mathbb{Z}_{\geq 0})}^2 \leq C^2 \max_n \#D_\varepsilon^n + C_\varepsilon^{-1} \left(\inf_{u \in \mathcal{U}^{1,2}} \mathcal{E}^a(u) + 1 \right) =: C_{\text{unif}} < \infty.$$

From the above, one can show that $\sup_n |u'_{n, \ell}| < \infty$ for each $\ell \in \mathbb{Z}_{\geq 0}$. By using this bound and a diagonalization argument as in proofs of the Arzela-Ascoli theorem, we can find a subsequence of $\{u'_n\}$ that converges pointwise to a $u'_\infty \in \ell^\infty(\mathbb{Z}_{\geq 0})$. For convenience, let us again assume that $\{u'_n\}$ has this property. This $u'_\infty \in \ell^2(\mathbb{Z}_{\geq 0})$. This can be shown through a proof by contradiction. If it weren't in $\ell^2(\mathbb{Z}_{\geq 0})$, then there would exist an index $L \in \mathbb{N}$ such that $\sum_{\ell=0}^L |u'_{\infty, \ell}|^2 > C_{\text{unif}}$. However, by the construction of the subsequence that converges pointwise to u_∞ , we must have that $\sum_{\ell=0}^L |u'_{n_k, \ell}|^2$ converges to $\sum_{\ell=0}^L |u'_{\infty, \ell}|^2$ for large enough k and thus converges to a

value greater than C_{unif} . This contradicts the uniform bound on the $\{u'_n\}$, so we must have that $u_\infty \in \mathcal{U}$ since we can simply set $u_{\infty,0} = 0$. Maintaining the assumption that $\{u'_n\}$ converges to u'_∞ pointwise, we may use Fatou's Lemma to show that

$$\begin{aligned} \inf_{u \in \mathcal{U}} \mathcal{E}^a(u) &= \liminf_{n \rightarrow \infty} \mathcal{E}^a(u_n) \\ &\geq \liminf_{n \rightarrow \infty} V^{\text{surf}}(u'_{n,0}) + \sum_{\ell=0}^{\infty} \liminf_{n \rightarrow \infty} V(u'_{n,\ell}, u'_{n,\ell+1}) \\ &= V^{\text{surf}}(u'_{\infty,0}) + \sum_{\ell=0}^{\infty} V(u'_{\infty,\ell}, u'_{\infty,\ell+1}) \\ &= \mathcal{E}^a(u_\infty) \geq \inf_{u \in \mathcal{U}} \mathcal{E}^a(u). \end{aligned}$$

Thus, u_∞ is an energy minimizing configuration of the atomistic energy \mathcal{E}^a in \mathcal{U} . \square

It should be noted that this theorem does not state that there exists only one energy-minimizing configuration. While for many systems it is reasonable and natural to expect that there exists a unique ground state, the assumptions given on the energy do not preclude the existence of multiple states for a system that achieve the same minimal energy value. In the following paragraphs, u_{gr}^a may refer to any ground state.

While the presence of surface effects prevent the explicit computation of the exact atomistic minimizers in the general case, the decay of these solutions can be examined. The decay of these solutions affect the degree of influence that surface behavior will have on the material's response. As we now prove, surface effects are highly localized in our model.

Theorem 2.1.2. *Let u_{gr}^a be a critical point of \mathcal{E}^a . Then, there exists $0 \leq \mu_a < 1$ such that*

$$|(u_{\text{gr}}^a)'_\ell| \lesssim \mu_a^\ell \quad \text{for all } \ell \in \mathbb{Z}_{\geq 0}.$$

Proof. Critical points of \mathcal{E}^a satisfy the Euler–Lagrange equation

$$\langle \delta \mathcal{E}^a(u'), v' \rangle = 0 \quad \text{for all } v \in \mathcal{U}.$$

Expanding the first variation $\delta\mathcal{E}^a(u')$ about $u' = 0$ yields

$$\langle \delta\mathcal{E}^a(0) + \delta^2\mathcal{E}^a(0)u' + \zeta(u'), v' \rangle = 0,$$

where $\zeta(u')$ is the remainder term from the expansion, which can be readily shown to satisfy the bounds

$$|\zeta_0| \lesssim |u'_0|^2 + |u'_1|^2 \quad \text{and} \quad |\zeta_\ell| \lesssim |u'_{\ell-1}|^2 + |u'_\ell|^2 + |u'_{\ell+1}|^2 \quad \text{for } \ell \geq 1. \quad (2.14)$$

The unlisted constants in these inequalities are the bounds on the third-order derivatives of the site energies which exist due to property (ii). We may explicitly compute the remaining terms in the Taylor series expansion keeping in mind that $V(F, F)$ achieves its minimum at $(0, 0)$:

$$\begin{aligned} \langle \delta\mathcal{E}^a(0), v' \rangle &= v'_0 \left\{ \partial_F V^{\text{surf}}(0) \right\} \quad \text{and} \\ \langle \delta^2\mathcal{E}^a(0)u', v' \rangle &= v'_0 u'_0 \left\{ \partial_F^2 V^{\text{surf}}(0) + \partial_{11}^2 V(0, 0) \right\} + v'_0 u'_1 \left\{ \partial_{12}^2 V(0, 0) \right\} \\ &+ \sum_{\ell=1}^{\infty} v'_\ell \left[u'_{\ell-1} \left\{ \partial_{12}^2 V(0, 0) \right\} + u'_\ell \left\{ \partial_{22}^2 V(0, 0) + \partial_{11}^2 V(0, 0) \right\} \right. \\ &\quad \left. + u'_{\ell+1} \left\{ \partial_{12}^2 V(0, 0) \right\} \right]. \end{aligned}$$

From these computations, we see that a solution u' to the atomistic problem must be a solution to the following system of equations:

$$\left\{ \partial_{12}^2 V^{\text{bulk}}(0, 0) \right\} u'_{\ell+1} + \left\{ \partial_{22}^2 V(0, 0) + \partial_{11}^2 V(0, 0) \right\} u'_\ell + \left\{ \partial_{12}^2 V^{\text{bulk}}(0, 0) \right\} u'_{\ell-1} = -\zeta_\ell \quad (2.15)$$

for $\ell \geq 1$ with the boundary condition

$$\left\{ \partial_{11}^2 V^{\text{surf}}(0) + \partial_{11}^2 V(0, 0) \right\} u'_0 + \left\{ \partial_{12}^2 V(0, 0) \right\} u'_1 = -\zeta_0 - \left(\partial_F V^{\text{surf}}(0) \right) =: \tilde{\zeta}_0.$$

For readability, we define the following constants that we will use to rewrite the above

system of equations:

$$a := \partial_{11}^2 V(0, 0) + \partial_{22}^2 V(0, 0), \quad b := \partial_{12}^2 V(0, 0), \quad (2.16)$$

$$a_s := \partial_F^2 V^{\text{surf}}(0) + \partial_{11}^2 V(0, 0), \quad b_s := \partial_{12}^2 V(0, 0). \quad (2.17)$$

The system (2.15) can now be written as

$$a_s u'_0 + b u'_1 = \tilde{\zeta}_0, \quad (2.18)$$

$$b u'_{\ell+1} + a u'_\ell + b u'_{\ell-1} = -\zeta_\ell \quad \text{for } \ell \geq 1. \quad (2.19)$$

We now suppose that $b \neq 0$. The case when $b = 0$ is analogous. Solving for the homogeneous solution to this system of equations gives

$$u'_\ell = c_+ \lambda_+^\ell + c_- \lambda_-^\ell, \quad \text{where} \quad \lambda_\pm = \frac{-a \pm \sqrt{a^2 - 4b^2}}{2b}.$$

The positive definiteness of V from property (iv) implies that $a - 2b > 0$ and $a + 2b > 0$. Hence, the discriminant is always positive: $a^2 - 4b^2 > 0$. As a result, the above formula for λ_\pm provides two distinct values. Since we are considering the case when $b \neq 0$, $\lambda_\pm \neq 0$. The symmetry of the simple difference equation in Eq. (2.19) then implies that $\lambda_+ = 1/\lambda_-$. This relation combined with the fact that the discriminant is never 0 implies that $\lambda_\pm \neq 1$. Without loss of generality, then, we must have that $0 < |\lambda_+| < 1$ and $|\lambda_-| > 1$. As solutions to the atomistic problem must belong to \mathcal{U} , we require that $u'_\ell \rightarrow 0$ as $\ell \rightarrow \infty$. This boundary condition at infinity implies that $c_- = 0$ in order to prevent exponential growth in the strain. Thus, letting $\lambda := \lambda_+$, since the subscript no longer matters, we have that solutions of the homogeneous equation are of the form $u'_\ell = u'_0 \lambda^\ell$. A discrete Green's function argument provides the solution for the inhomogeneous equation:

$$u'_\ell = C_{\text{BC}} \lambda^\ell + D^{-1} \sum_{k=0}^{\infty} \lambda^{|\ell-k|} \zeta_k,$$

where $D := \sqrt{a^2 - 4b^2}$ and C_{BC} can be determined from u'_0 . Taking the absolute value

of both sides, using the triangle inequality, and applying (2.14), we can show that

$$|u'_\ell| \leq C_{\text{BC}}|\lambda|^\ell + D^{-1} \sum_{k=0}^{\infty} |\lambda|^{\ell-k} |\zeta_k| \lesssim C_{\text{BC}}|\lambda|^\ell + D^{-1} \sum_{k=0}^{\infty} |\lambda|^{\ell-k} |u'_k|^2.$$

Now, let μ be a constant such that $|\lambda| < \mu < (1 + |\lambda|)/2$. Then,

$$\sum_{m=0}^{\infty} \mu^{|\ell-m|} |u'_m| \lesssim \sum_{m=0}^{\infty} C_{\text{BC}} \mu^{|\ell-m|} |\lambda|^m + D^{-1} \sum_{m,k \geq 0} \mu^{|\ell-m|} |\lambda|^{|m-k|} |u'_k|^2.$$

Observe that

$$\sum_{m=0}^{\infty} \mu^{|\ell-m|} |\lambda|^{|m-k|} \lesssim \mu^{|\ell-k|},$$

where the ignored coefficient depends solely on λ . Then, from the above, we have that

$$\sum_{m=0}^{\infty} \mu^{|\ell-m|} |u'_m| \lesssim C_{\text{BC}} \mu^\ell + D^{-1} \sum_{k=0}^{\infty} \mu^{|\ell-k|} |u'_k|^2. \quad (2.20)$$

Ignoring the prefactor D^{-1} , the second term on the right-hand side of (2.20) can be bounded by

$$\sum_{k=0}^{\infty} \mu^{|\ell-k|} |u'_k|^2 = \sum_{k \leq k_0} \mu^{|\ell-k|} |u'_k|^2 + \sum_{k \geq k_0} \mu^{|\ell-k|} |u'_k|^2 \lesssim \mu^\ell + \sup_{k \geq k_0} |u'_k| \sum_{k \geq k_0} \mu^{|\ell-k|} |u'_k|,$$

where we have used the fact that $\|u'\|_{\ell^\infty}^2 < \infty$ since $u \in \mathcal{U}$. For any $\varepsilon > 0$, we can choose k_0 sufficiently large so that $\sup_{k \geq k_0} |u'_k| \leq \varepsilon$. This inequality then becomes

$$D^{-1} \sum_{k=0}^{\infty} \mu^{|\ell-k|} |u'_k|^2 \lesssim \mu^\ell + \varepsilon \sum_{k \geq k_0} \mu^{|\ell-k|} |u'_k|.$$

Substituting this bound into (2.20) yields

$$(1 - \varepsilon) |u'_\ell| \leq (1 - \varepsilon) \sum_{k=0}^{\infty} \mu^{|\ell-k|} |u'_k| \lesssim \mu^\ell.$$

Finally, we have the desired result:

$$|u'_\ell| \lesssim \mu^\ell. \quad \square$$

Surface effects, then, are extremely concentrated at the surface of the system. This result implies the existence of two scales within the problem and motivates the approach of solving the atomistic problem by considering separately the bulk and surface responses that will be considered in Chapter 4. In addition, the exponential decay of the strain due to surface effects justifies ignoring surface effects in very large systems as is usually the case.

We now proceed to incorporating external forces into the analysis and prove the existence of solutions in the presence of applied forces. To that end, we begin by assuming that a ground state u_{gr}^{a} is strongly stable; that is, we suppose that there exists an atomistic stability constant $c_{\text{a}} > 0$ such that

$$\langle \delta^2 \mathcal{E}^{\text{a}}(u_{\text{gr}}^{\text{a}})v, v \rangle \geq c_{\text{a}} \|v'\|_{\ell^2(\mathbb{Z}_{\geq 0})}^2 \quad \text{for all } v \in \mathcal{U}. \quad (2.21)$$

This stability assumption on u_{gr}^{a} enables us to prove the existence of nearby strongly stable local minimizers of the atomistic problem from (2.5) with small external forces. We define an element $u^{\text{a}} \in \mathcal{U}$ to be a strongly stable solution to the atomistic problem if and only if it satisfies the Euler-Lagrange equation

$$\langle \delta \mathcal{E}^{\text{a}}(u^{\text{a}}), v \rangle = \langle f, v \rangle \quad \text{for all } v \in \mathcal{U}$$

as well as the stability condition

$$\langle \delta^2 \mathcal{E}^{\text{a}}(u^{\text{a}})v, v \rangle \geq c \|v'\|_{\ell^2(\mathbb{Z}_{\geq 0})}^2 \quad \text{for all } v \in \mathcal{U}, \quad (2.22)$$

for some constant $c > 0$. The exact form of the first and second variations of \mathcal{E}^{a} for the general atomistic energy are provided in Propositions A.1.1 and A.1.2.

Corollary 2.1.3. *There exist $\varepsilon, C > 0$ such that, for all $f \in \mathcal{U}^*$ with $\|f\|_{\mathcal{U}^*} < \varepsilon$, the atomistic problem (2.5) has a unique, strongly-stable solution with $\|(u^{\text{a}} - u_{\text{gr}}^{\text{a}})'\|_{\ell^2} \leq C \|f\|_{\mathcal{U}^*}$.*

Proof. This is an immediate consequence of the inverse function theorem (Theorem A.2.1). \square

This result implies that the atomistic problem (2.5) is well-defined for small dead-load forces. In the next section, we discuss the Cauchy–Born approximation to this atomistic model.

2.2 Cauchy–Born Model

A common approach to determining the approximate bulk behavior of perfect crystalline materials involves the utilization of the Cauchy–Born model of atomistic interactions. The Cauchy–Born model approximates the non-local interactions amongst the constituents in an atomistic system with a local approximation. A limiting procedure then turns the discrete problem into a continuum one [13]. Applying this approach to our atomistic problem from above, we find that the Cauchy–Born energy approximation for the semi-infinite chain model is

$$\mathcal{E}^{\text{cb}}(u) := \int_0^\infty W(\nabla u(x)) dx \quad \text{for } u \in \mathcal{U}^{\text{cb}}, \quad (2.23)$$

where $W(F) := V(F, F)$ is the Cauchy–Born energy density function and the space of permissible displacements is given by

$$\mathcal{U}^{\text{cb}} := \{u \in H_{\text{loc}}^1(0, \infty) \mid \nabla u \in L^2(0, \infty) \text{ and } u(0) = 0\}.$$

We note that the Cauchy–Born energy density function W inherits the smoothness of the bulk site energy. As a result, $W \in C^3(\mathbb{R})$. For clarity, derivatives of W with respect to its argument as opposed to x will be indicated by $\partial_F W$. We also note that the space \mathcal{U} may be considered a subspace of \mathcal{U}^{cb} if we identify the lattice functions $u \in \mathcal{U}$ with their piecewise continuous interpolants.

2.2.1 Inconsistency of Cauchy–Born Method

An important feature of the Cauchy–Born method of approximation is that for atomistic systems without defects, the Cauchy–Born approximation and the exact model agree

for homogeneous deformations. In systems containing defects such as surfaces, however, this property is lost. In the above energy, this discrepancy arises due to the loss of a distinct surface term in the energy. The Cauchy–Born model treats every point in the chain as an interior point. The absence of a surface component to the energy results in an $\mathcal{O}(1)$ error in the consistency estimate for the Cauchy–Born model as compared to the atomistic system. We demonstrate this error in the case of zero external forces, or $f = 0$. In this case, the energy-minimizing configuration for the Cauchy–Born system is clearly $u^{\text{cb}} = 0$ as can be seen using properties (iii)–(v) of the site energies and the definition of W . We now show that there can be no convergence of the Cauchy–Born approximate ground state and the atomistic result.

Proposition 2.2.1. *The unique minimizer of \mathcal{E}^{cb} in \mathcal{U}^{cb} is $u^{\text{cb}} = 0$. Its atomistic residual is bounded by*

$$\sup_{v \in \mathcal{U}, \|v'\|_{\ell^2(\mathbb{Z}_{\geq 0})} = 1} |\langle \delta \mathcal{E}^{\text{a}}(0), v \rangle| = \|\delta \mathcal{E}^{\text{a}}(0)\|_{\mathcal{U}^*} = |\partial_F V^{\text{surf}}(0)|.$$

In particular, $\|(u_{\text{gr}}^{\text{a}} - u^{\text{cb}})'\|_{\ell^2} \geq M^{-1} |\partial_F V^{\text{surf}}(0)|$, where M is the global Lipschitz constant of $\delta \mathcal{E}^{\text{a}}$.

Proof. Let $u = 0$. Then, properties (iii)–(v) imply that $\delta \mathcal{E}^{\text{a}}(u)$ is given by

$$\begin{aligned} \langle \delta \mathcal{E}^{\text{a}}(u), v \rangle &= v'_0 \left\{ \partial_F V^{\text{surf}}(u'_0) + \partial_1 V(u'_0, u'_1) \right\} + \sum_{\ell=1}^{\infty} v'_\ell \left\{ \partial_2 V(u'_{\ell-1}, u'_\ell) + \partial_1 V(u'_\ell, u'_{\ell+1}) \right\} \\ &= v'_0 \partial_F V^{\text{surf}}(0). \end{aligned}$$

We can maximize this result by taking $v'_0 = \text{sign}(\partial_F V^{\text{surf}}(0))$ and setting $v'_\ell = 0$ for all $\ell > 0$. Clearly, such a $v \in \mathcal{U}$. Thus, we have that

$$\|\delta \mathcal{E}^{\text{a}}(0)\|_{\mathcal{U}^*} = |\partial_F V^{\text{surf}}(0)|$$

as desired.

To prove the lower bound on the error, we simply note that

$$|\partial_F V^{\text{surf}}(0)| = \|\delta \mathcal{E}^{\text{a}}(0)\|_{\mathcal{U}^*} = \|\delta \mathcal{E}^{\text{a}}(0) - \delta \mathcal{E}^{\text{a}}(u_{\text{gr}}^{\text{a}})\|_{\mathcal{U}^*} \leq M \|(u^{\text{cb}} - u_{\text{gr}}^{\text{a}})'\|_{\ell^2},$$

where we have used the fact that the first variation in the atomistic energy is Lipschitz continuous. \square

In general, we expect that $|\partial_F V^{\text{surf}}(0)| \neq 0$ since we lack the symmetry in interactions at the surface site that is present in the interior. In addition, this term will not vanish in the usual scaling limit as the atomic spacing is sent to zero. This consistency error combined with the Lipschitz continuity of the first variation of the atomistic energy implies that we cannot prove any sort of convergence between the Cauchy–Born and atomistic solutions in this space [24]. As expected, the Cauchy–Born and atomistic energy-minimizing configurations are not in agreement because of surface effects.

This lack of convergence of the Cauchy–Born method to the atomistic method shows that the Cauchy–Born method cannot serve as an accurate approximation to the fully atomistic system when studying surface effects. However, there may be means of modifying the Cauchy–Born method in order to capture these missed surface effects while still maintaining the efficiency of the method. This possibility is made more promising due to the result in Theorem 2.1.2 as we have shown that surface effects are a highly localized phenomenon in our atomistic model.

In later chapters, we will explore two possible modifications of the Cauchy–Born method to improve the method. In the next chapter, we will discuss the introduction of a surface integral that represents a continuum approximation of these missed surface effects following the spirit of the original Cauchy–Born approximation. Afterwards, we will discuss a predictor–corrector method that uses the Cauchy–Born method as an approximation for the bulk behavior of the material followed by a correction to account for surface effects. It will be shown that the bulk and surface effects decouple so that a concurrent coupling scheme is not required to capture these effects. A post-processing of the Cauchy–Born solution will suffice.

2.2.2 Existence and Regularity of Cauchy–Born Solutions

We are, therefore, still interested in the Cauchy–Born method and its approximation to the atomistic surface problem. Precisely, we are interested in finding the solutions

$$u^{\text{cb}} \in \arg \min \{ \mathcal{E}^{\text{cb}}(u) - \langle f, u \rangle_{\mathbb{R}_+} \mid u \in \mathcal{U}^{\text{cb}} \}, \quad (2.24)$$

where we identify the lattice function f with its continuous piecewise affine interpolant and $\langle f, u \rangle_{\mathbb{R}_+} := \int_0^\infty f u \, dx$. It is easy to see that $f \in \mathcal{U}^*$ implies that $\langle f, \cdot \rangle_{\mathbb{R}_+} \in (\mathcal{U}^{\text{cb}})^*$. We show this in Lemma 2.2.2.

Analogously to the atomistic problem, we say u^{cb} is a strongly stable solution to (2.24) if it satisfies the first-order and strong second-order optimality conditions:

$$\begin{aligned} \langle \delta \mathcal{E}^{\text{cb}}(u^{\text{cb}}), v \rangle &= \langle f, v \rangle_{\mathbb{R}_+} \quad \text{for all } v \in \mathcal{U}^{\text{cb}} \quad \text{and} \\ \langle \delta^2 \mathcal{E}^{\text{cb}}(u^{\text{cb}})v, v \rangle &\geq c_{\text{cb}} \|\nabla v\|_{L^2([0, \infty))}^2 \quad \text{for all } v \in \mathcal{U}^{\text{cb}} \end{aligned} \quad (2.25)$$

for some constant $c_{\text{cb}} > 0$. This c_{cb} is the Cauchy–Born stability constant. The exact forms of the first and second variations of the Cauchy–Born energy may be found in Propositions A.1.1 and A.1.2.

For small enough external forces, we can again guarantee the existence of strongly stable solutions to the Cauchy–Born problem and deduce some additional facts concerning the regularity of these solutions. Before that, however, we first derive an alternative form for the energy contribution from the applied forces in terms of the strain rather than the displacement. This will be useful in proofs later on.

The reformulation of the energy contribution due to the external forces is analogous to that done for the atomistic case and will be accomplished using integration by parts. Recall in the atomistic case that $f \in \mathcal{U}^*$ if and only if there exists $g \in \ell^2(\mathbb{Z}_{\geq 0})$ such that $\langle f, u \rangle = \langle g, u' \rangle$. Setting $g_{-1} = 0$, we may use a discrete summation by parts to show that

$$f_\ell = g_\ell - g_{\ell-1}. \quad (2.26)$$

Conversely, if we are given f , we may recover g via

$$g_\ell := \sum_{k=\ell+1}^{\infty} f_k := \lim_{K \rightarrow \infty} \sum_{k=\ell+1}^K f_k. \quad (2.27)$$

In the Cauchy–Born model, we identify f with its piecewise-affine interpolant. The continuous analogue of (2.27) is

$$\tilde{g}(x) := \int_x^\infty f(s) \, ds := \lim_{K \rightarrow \infty} \int_x^K f(s) \, ds. \quad (2.28)$$

Lemma 2.2.2. *Let $f \in \mathcal{U}^*$. Then, g and \tilde{g} are well-defined and satisfy*

$$|g_\ell - \tilde{g}(\ell + 1/2)| = \frac{1}{8}|f'_\ell| \quad \text{for all } \ell \in \mathbb{Z}_{\geq 0}, \quad \text{and} \quad (2.29)$$

$$|\tilde{g}(x)| \lesssim \sum_{m=\ell-1}^{\ell+1} |g_m| \quad \text{for all } x \in [\ell, \ell + 1]. \quad (2.30)$$

Proof. Since $f \in \mathcal{U}^*$, there exists $g \in \ell^2$ such that (2.26) holds as shown above. Let $M > \ell + 1$. Then,

$$\sum_{m=\ell+1}^M f_m = \sum_{m=\ell+1}^M (g_{\ell-1} - g_\ell) = g_\ell - g_M$$

In the limit as $M \rightarrow \infty$, we then have that

$$\sum_{m=\ell+1}^M f_m \rightarrow g_\ell.$$

Hence, (2.27) is well-defined.

Similarly, let $M \in \mathbb{Z}$ and $M > \ell + 1$. Then,

$$\begin{aligned} \int_{\ell+1/2}^M f(s) ds - \sum_{m=\ell+1}^M f_m &= \int_{\ell+1/2}^{\ell+1} f(s) ds + \int_{\ell+1}^M f(s) ds - \sum_{m=\ell+1}^M f_m \\ &= \frac{1}{2} \left[\frac{1}{2} (\frac{1}{2}(f_\ell + f_{\ell+1}) + f_{\ell+1}) \right] \\ &\quad + \sum_{m=\ell+1}^{M-1} \left[\frac{1}{2}(f_m + f_{m+1}) - f_m \right] - f_M \\ &= \frac{1}{8}(f_\ell - f_{\ell+1}) - \frac{1}{2}f_M \end{aligned}$$

Taking the limit as $M \rightarrow \infty$, we may use the definitions of g and \tilde{g} to show that

$$|g_\ell - \tilde{g}(\ell + 1/2)| = \frac{1}{8}|f_\ell - f_{\ell+1}|$$

By defining $f'_\ell := f_\ell - f_{\ell+1}$, we arrive at the first result (2.29) in the lemma. We can also conclude from this approach that $\tilde{g}(x)$ is well-defined for all x .

To prove the second estimate, we simply note that, for $x \in [\ell, \ell + 1]$,

$$|\tilde{g}(x) - \tilde{g}(\ell + 1/2)| = \left| \int_{\ell+1/2}^x f(s) ds \right| \lesssim |f_\ell| + |f_{\ell+1}|,$$

and then apply (2.26). \square

With the above lemma proven, we now return our consideration to the existence and regularity of solutions to the Cauchy–Born problem.

Theorem 2.2.3. *There exists $\varepsilon_{\text{cb}} > 0$ such that for all $f \in \mathcal{U}^*$ with $\|f\|_{\mathcal{U}^*} < \varepsilon_{\text{cb}}$, a strongly stable solution $u^{\text{cb}} \in \mathcal{U}^{\text{cb}}$ of the Cauchy–Born problem (2.24) exists.*

Moreover, $u^{\text{cb}} \in H_{\text{loc}}^3$, and it satisfies the bounds

$$|\nabla u^{\text{cb}}(0)| \lesssim \|f\|_{\mathcal{U}^*}, \quad |\nabla^2 u^{\text{cb}}(x)| \lesssim |f(x)|, \quad \text{and} \quad |\nabla^3 u^{\text{cb}}(x)| \lesssim |\nabla f(x)| + |f(x)|^2.$$

In addition, we prove that

$$|\nabla u^{\text{cb}}(x)| \lesssim |\tilde{g}(x)|, \tag{2.31}$$

where \tilde{g} is as defined in (2.28).

Proof. To begin with, we note that throughout this proof, ∇ will always refer to the gradient with respect to x . The Euler–Lagrange equation of the Cauchy–Born problem from (2.24) can be written as

$$-\nabla[\partial_F W(\nabla u)] = f. \tag{2.32}$$

We now consider the behavior of this system at $x = \infty$. Since we are considering elements $u \in \mathcal{U}^{\text{cb}}$, $\nabla u(x) \rightarrow 0$ as $x \rightarrow \infty$.

The derivative $\partial_F W(F)$ is continuous and $\partial_F W(0) = 0$ due to site energy properties (iii) and (v), so $\lim_{x \rightarrow \infty} \partial_F W(\nabla u) = 0$. Thus, we may integrate (2.32) from x to ∞ making use of this boundary condition to show that

$$\partial_F W(\nabla u) = \int_x^\infty f(s) ds = \tilde{g}(x).$$

As f was defined to be piecewise continuous, it is also clear that $f(x) = -\nabla \tilde{g}(x)$ almost everywhere. We now seek to use the elementary inverse function theorem in order to

solve for ∇u . First, observe that there exists a $G > 0$ such that $\partial_F^2 W(F) > \frac{1}{2} \partial_F^2 W(0) > 0$ on $[-G, G]$. This follows immediately from site energy properties (iv) and (i). Thus, $\partial_F W(F)$ is strictly monotone on this interval. Provided that $\tilde{g}([0, \infty)) \subset \partial_F W([-G, G])$, which can be guaranteed for small f , we may now use the inverse function theorem to show that

$$\nabla u(x) = (\partial_F W)^{-1}(\tilde{g}(x))$$

is a solution to the Cauchy–Born problem, where $(\partial_F W)^{-1} : \partial_F W([-G, G]) \rightarrow [-G, G]$ is the inverse of $\partial_F W$ on the given domain. Due to the restriction on the range of the inverse function, $\nabla u(x) \in [-G, G]$ so that it is easy to see that the solution must be stable with a stability constant $c_{\text{cb}} \geq \frac{1}{2} \partial_F^2 W(0)$. It is easy to show with this that $(\partial_F W)^{-1}$ is Lipschitz continuous. Noting that $(\partial_F W)^{-1}(0) = 0$, Lipschitz continuity then yields the bound

$$|\nabla u^{\text{cb}}(x)| = |(\partial_F W)^{-1}(\tilde{g}(x)) - (\partial_F W)^{-1}(0)| \lesssim |\tilde{g}(x)| = \left| \int_x^\infty f(x) dx \right|,$$

where we have ignored the Lipschitz constant for the inverse function. The derivative ∇u inherits the smoothness of \tilde{g} since $\partial_F W(F) \in C^2(\mathbb{R})$. In particular, ∇u is continuous everywhere and differentiable almost everywhere. As we have an explicit expression for ∇u , we may compute its derivative to find the following bound:

$$|\nabla^2 u(x)| = \left| -\frac{f(x)}{\partial_F^2 W(\nabla u(x))} \right| \leq \frac{|f(x)|}{c_{\text{cb}}}.$$

Thus, we have shown two of the three proposed bounds. To show the final bound on the third derivative, we note that $\partial_F^2 W(F)$ is once more differentiable and that f is differentiable on $[0, \infty) \setminus \mathbb{Z}_{>0}$. Thus, we may compute the derivative of $\nabla^2 u^{\text{cb}}(x)$ explicitly to show that $\nabla^3 u^{\text{cb}}$ exists almost everywhere. This computed derivative may then be bounded:

$$|\nabla^3 u(x)| = \left| -\frac{\nabla f(x)}{\partial_F^2 W(\nabla u(x))} + \frac{f(x)}{\partial_F^2 W(\nabla u(x))^2} \partial_F^3 W(\nabla u(x)) \nabla^2 u(x) \right| \lesssim \frac{|\nabla f(x)|}{c_{\text{cb}}} + \frac{|f(x)|^2}{c_{\text{cb}}^2},$$

where we have ignored the constant that comes from the bound on $\partial_F^3 W(F)$ by site energy property (ii). This shows that $\nabla^3 u^{\text{cb}}$ is Lebesgue integrable. The absolute

continuity of $\nabla^2 u^{\text{cb}}$ then follows immediately from observing that the first fundamental theorem of calculus holds true for $\nabla^3 u^{\text{cb}}(x)$. This completes the proof. \square

As the Cauchy–Born and atomistic solutions belong to different spaces, they cannot be directly compared. Earlier, when the inconsistency of the Cauchy–Born model was examined, we simply assumed that $0 \in \mathcal{U}^{\text{cb}}$ should correspond with $0 \in \mathcal{U}$. While that is quite reasonable in that specific case, comparing non-zero solutions requires a different approach. To that end, we introduce a projection operator $\Pi_a : \mathcal{U}^{\text{cb}} \rightarrow \mathcal{U}$ via

$$(\Pi_a u)_0 = 0 \quad \text{and} \quad (\Pi_a u)'_\ell = \int_\ell^{\ell+1} \nabla u(s) ds \quad \text{for } \ell \in \mathbb{Z}_{\geq 0}, u \in \mathcal{U}^{\text{cb}}. \quad (2.33)$$

We verify that $\Pi_a u^{\text{cb}} \in \mathcal{U}$ below. Other projection operators may be chosen as well without affecting the results of this work; the choice made here is simply convenient. Next, we recall an auxiliary result that allows us to reduce the continuous Cauchy–Born model to a discrete model. To that end, we recall that we can identify discrete test functions $v \in \mathcal{U}$ with continuous test functions $v \in \mathcal{U}^{\text{cb}}$ via piecewise affine interpolation. Through the same identification, we can also admit $u \in \mathcal{U}$ as arguments for $\delta\mathcal{E}^{\text{cb}}$.

Proposition 2.2.4. *Under the conditions of Theorem 2.2.3, we have $\Pi_a u^{\text{cb}} \in \mathcal{U}$, and*

$$|\langle \delta\mathcal{E}^{\text{cb}}(u^{\text{cb}}) - \delta\mathcal{E}^{\text{cb}}(\Pi_a u^{\text{cb}}), v \rangle| \lesssim \|\nabla^2 u^{\text{cb}}\|_{L^4}^2 \|\nabla v\|_{L^2} \quad \text{for all } v \in \mathcal{U}.$$

Proof. The inequality is a simplified variant of [24, Lemma 5.2]. To show that $\Pi_a u^{\text{cb}}$ belongs to \mathcal{U} , we need only show that $(\Pi_a u^{\text{cb}})' \in \ell^2$ since $(\Pi_a u)_0 := 0$. Using Theorem 2.2.3, the continuity of \tilde{g} , Lemma 2.2.2, and the fact that $g \in \ell^2$, we find that

$$\begin{aligned} \sum_{\ell=0}^{\infty} |(\Pi_a u^{\text{cb}})'_\ell|^2 &= \sum_{\ell=0}^{\infty} \left| \int_\ell^{\ell+1} \nabla u(s) ds \right|^2 \lesssim \sum_{\ell=0}^{\infty} \left| \int_\ell^{\ell+1} \tilde{g}(s) ds \right|^2 \\ &\leq \sum_{\ell=0}^{\infty} \left[\max_{x \in [\ell, \ell+1]} \tilde{g}(x) \right]^2 \lesssim \sum_{\ell=0}^{\infty} \left[\sum_{m=\ell-1}^{\ell+1} |g_m| \right]^2 < \infty. \end{aligned}$$

Thus, $\Pi_a u^{\text{cb}} \in \mathcal{U}$. \square

Chapter 3

Surface Cauchy–Born Method

As shown in Proposition 2.2.1, the Cauchy–Born method is unable to accurately approximate the atomistic system with a surface. The surface Cauchy–Born (SCB) method seeks to address this issue through a modification of the Cauchy–Born method. Specifically, the surface Cauchy–Born method introduces a surface energy integral to the Cauchy–Born energy in order to capture the missed effects. For the 1D chain, this correction manifests simply as an additional surface energy function. The surface Cauchy–Born approximation to the ground state of the atomistic system is then computed using the usual energy-minimization approach in the variational formulation. The surface energy correction in the SCB method naturally allows for size-dependent effects as the relative importance of the Cauchy–Born energy and the surface correction vary according to the size of the system under investigation. In this chapter, we develop the surface Cauchy–Born method for our surface problem and analyze the accuracy of the approximation under the finite-element method in certain physical limits.

Recall that the Cauchy–Born energy for the given problem is the following:

$$\mathcal{E}^{\text{cb}}(u) := \int_0^\infty W(\nabla u(x)) dx \quad \text{for } u \in \mathcal{U}^{\text{cb}},$$

where $W(F) := V(F, F)$ is the Cauchy–Born stored energy density function. Note that the continuum Cauchy–Born model fails to distinguish between the energy densities at the surface and the interior of the material. This is indicative of the failure of the regular Cauchy–Born approximation to capture the surface effects that are present in

the atomistic system. The surface Cauchy–Born model seeks to rectify this deficiency through the addition of a surface energy term which we will denote by γ . In the continuum description, the surface Cauchy–Born energy may be written as

$$\mathcal{E}^{\text{scb}}(u) := \mathcal{E}^{\text{cb}}(u) + \gamma(\nabla u(0)),$$

where we have written the surface energy in terms of the strain at the surface and γ has yet to be defined. Following the motivation for the original Cauchy–Born approximation for the bulk, the surface energy introduced in the SCB model is chosen in such a way that the SCB energy and the atomistic energy agree for homogeneous deformations. Therefore, we may compute the surface energy by considering the following:

$$\mathcal{E}^{\text{a}}(F) = \mathcal{E}^{\text{scb}}(F) = \mathcal{E}^{\text{cb}}(F) + \gamma(F),$$

where F indicates a constant strain. Computing γ in this way, we find that

$$\gamma(F) = V^{\text{surf}}(F) - \frac{1}{2}V(F, F) = V^{\text{surf}}(F) - \frac{1}{2}W(F).$$

As a result, $\gamma \in C^3(\mathbb{R})$. Note that this correction is best understood through the lens of the site energy description of the chain. This surface energy corrects for the fact that the atom at the end of the chain only has one neighbor instead of two like the rest of the atoms in the chain. This correction will only affect the longer-range portion of the interactions. For purely nearest-neighbor interactions, their contributions to γ will cancel. This is due to the fact that nearest-neighbor interactions are in some sense already local, so their behavior is well-approximated by the regular Cauchy–Born method even at surfaces. The longer-range and many-body interactions are the source of the difficulty for the Cauchy–Born method’s approximation of surface effects.

We now consider a P_0 finite-element discretization of the Cauchy–Born model in terms of the displacement gradient ∇u . Define $X_h := \{X_0, X_1, \dots\} \subset \mathbb{Z}_{\geq 0}$ to be a strictly increasing sequence of grid points with $X_0 := 0$. Define $h_j := X_{j+1} - X_j$ for all $j \geq 0$. We let $U_j' \subset \mathbb{R}$ denote the displacement gradient in our interpolation over the

element (X_j, X_{j+1}) . In this finite-element discretization,

$$\mathcal{E}_h^{\text{cb}}(U') := \sum_{j=0}^{\infty} h_j W(U'_j). \quad (3.1)$$

The surface Cauchy–Born energy for the finite element discretization of the problem is defined to be

$$\mathcal{E}_h^{\text{scb}}(U') := \mathcal{E}_h^{\text{cb}}(U') + \gamma(U'_0).$$

Setting $\mathcal{E}^{\text{a}}(F) = \mathcal{E}_h^{\text{scb}}(F)$ and solving for the surface correction energy as required by the surface Cauchy–Born method will yield the same function as in the continuum case. Therefore, γ will be used for the surface energy correction function for both the continuum and discretized descriptions.

For the analysis, we are interested in the first and second variations of the surface Cauchy–Born method. For consistency, derivatives of the surface correction term γ will be denoted using the same notation as for W . The first derivative of $\gamma(F)$ will be denoted by $\partial_F \gamma(F)$ and so on.

Proposition 3.0.5. $\mathcal{E}_h^{\text{cb}}$ and hence $\mathcal{E}_h^{\text{scb}}$ are well defined and twice Fréchet differentiable in the weighted-space $\ell_h^2(X_h)$ equipped with the norm

$$\|V'\|_{\ell_h^2} := \sum_{j=0}^{\infty} h_j |V'_j|^2.$$

The first and second variations of $\mathcal{E}_h^{\text{scb}}$ are given by

$$\begin{aligned} \langle \delta \mathcal{E}_h^{\text{scb}}(U'), V' \rangle &= \sum_{j=0}^{\infty} h_j \partial_F W(U'_j) V'_j + \partial_F \gamma(U'_0) V'_0, \\ \langle \delta^2 \mathcal{E}_h^{\text{scb}}(U') S', V' \rangle &= \sum_{j=0}^{\infty} h_j \partial_F^2 W(U'_j) S'_j V'_j + \partial_F^2 \gamma(U'_0) S'_0 V'_0. \end{aligned}$$

Proof. The energy function $\mathcal{E}_h^{\text{scb}} : \ell_h^2(X_h) \rightarrow \mathbb{R}$ is Fréchet differentiable if

$$\lim_{V' \rightarrow 0} \frac{|\mathcal{E}_h^{\text{scb}}(U' + V') - \mathcal{E}_h^{\text{scb}}(U') - \langle \delta \mathcal{E}_h^{\text{scb}}(U'), V' \rangle|}{\|V'\|_{\ell_h^2}} = 0$$

To show this quickly, observe that we may use Taylor's theorem to show the following:

$$\gamma(U'_0 + V'_0) = \gamma(U'_0) + \partial_F \gamma(U'_0) V'_0 + \partial_F^2 \gamma(\eta'_0) |V'_0|^2$$

and

$$W(U'_j + V'_j) = W(U'_j) + \partial_F W(U'_j) V'_j + \partial_F^2 W(\xi'_j) |V'_j|^2.$$

The above set of equations gives an expansion for each term in the SCB summation for $\mathcal{E}_h^{\text{scb}}(U' + V')$. Moreover, the first two terms in the Taylor series expansion cancel with their corresponding entries in the energies $\mathcal{E}_h^{\text{scb}}(U'_j)$ and $\langle \mathcal{E}_h^{\text{scb}}(U'_j), V'_j \rangle$ leaving only the remainder terms from the Taylor series expansions. Using the fact that the derivatives of the site energy functions are bounded, we easily see that

$$|\mathcal{E}_h^{\text{scb}}(U' + V') - \mathcal{E}_h^{\text{scb}}(U') - \langle \delta \mathcal{E}_h^{\text{scb}}(U'), V' \rangle| \lesssim \|V'\|_{\ell_h^2}^2.$$

Hence, the necessary limit is indeed 0. A similar computation shows that $\delta \mathcal{E}_h^{\text{scb}}(U')$ is Fréchet differentiable so that $\mathcal{E}_h^{\text{scb}}(U')$ is twice Fréchet differentiable. The proof of the Fréchet differentiability of $\mathcal{E}_h^{\text{cb}}$ follows immediately from the differentiability of $\mathcal{E}_h^{\text{scb}}$. \square

3.1 Analysis of the Linearized Systems

Recall that the ground state for the Cauchy–Born model is simply the zero strain state and that $W(F)$ achieves its minimum for $F = 0$. It is clear, then, that the discretized Cauchy–Born energy $\mathcal{E}_h^{\text{cb}}(U')$ is minimized by setting

$$(U^{\text{cb}})'_j = 0 \quad \text{for all } j = 0, 1, 2, \dots$$

In this chapter, as in the previous, superscripts will be used to denote ground state strains with capitals denoting a strain for a discretized system. We also note that these displacement gradients for the discretized Cauchy–Born model completely describe the exact ground state of the system as the endpoint of the chain of atoms under consideration will still be held fixed, or equivalently, $(U^{\text{cb}})_0 = 0$.

We now seek to determine the ground states of the other two models for comparison. As we expect the Cauchy–Born model to be a somewhat reasonable approximation to

the atomistic and surface Cauchy–Born models, we will find approximations to the ground states of these two systems by linearizing their equilibrium equations about the Cauchy–Born ground state. The force-balance equations for the atomistic and surface Cauchy–Born systems in the absence of external forces are respectively

$$\mathcal{F}^a(u') = \mathbf{0} \quad \text{and} \quad \mathcal{F}_h^{\text{scb}}(U') = \mathbf{0},$$

where

$$\mathcal{F}^a(u') := -\delta\mathcal{E}^a(u') \quad \text{and} \quad \mathcal{F}_h^{\text{scb}}(U') := -\delta\mathcal{E}_h^{\text{scb}}(U')$$

and $\mathbf{0}$ is an infinite-dimensional 0 vector. These equilibrium equations linearized about the Cauchy–Born ground state yield the following systems of equations:

$$\delta\mathcal{E}^a(0) + \delta^2\mathcal{E}^a(0)u' = \mathbf{0} \quad \text{and} \quad \delta\mathcal{E}_h^{\text{scb}}(0) + \delta^2\mathcal{E}_h^{\text{scb}}(0)U' = \mathbf{0}. \quad (3.2)$$

Extracting the relevant vectors from Proposition 3.0.5 and recalling that $\partial_F W(0) = 0$ from site energy property (iii), we see that the minimizing strain vector of the surface Cauchy–Born energy satisfies the following linear system:

$$\begin{aligned} \partial_F \gamma(0) + (h_0 \partial_F^2 W(0) + \partial_F^2 \gamma(0))U'_0 &= 0, \\ h_j \partial_F^2 W(0)U'_j &= 0 \quad \text{for } j = 1, 2, \dots \end{aligned}$$

Since $\partial_F^2 W(0) > 0$ by site energy property (iv), the linearized surface Cauchy–Born solution is given by

$$(U^{\text{scb}})'_0 = \frac{-\partial_F \gamma(0)}{h_0 \partial_F^2 W(0) + \partial_F^2 \gamma(0)} \quad \text{and} \quad (U^{\text{scb}})'_j = 0 \quad \text{for } j = 1, 2, \dots \quad (3.3)$$

provided that $h_0 \partial_F^2 W(0) + \partial_F^2 \gamma(0) \neq 0$, which we expect in general.

From the work in Theorem 2.1.2, we see that the atomistic solution to the linearized problem is simply

$$(u^a)'_\ell = u'_0 \lambda^\ell, \quad \text{where} \quad u'_0 = \frac{-\partial_F V^{\text{surf}}(0)}{a_s + b\lambda}, \quad \text{and} \quad \lambda = \frac{-a + \sqrt{a^2 - 4b^2}}{2b},$$

with a, b , and a_s as defined in Eq. (2.16). The exponential behavior of the surface effects

in this linearized model is dictated entirely by λ . It will be shown that $\lambda \in (-1, 1)$. We draw attention in particular to the fact that λ can be negative so that the sign of $(u^a)'_\ell$ can alternate. We note that we can rewrite λ as

$$\lambda = \frac{-1 + \sqrt{1 - \eta^2}}{\eta}, \quad \text{where} \quad \eta := \frac{2b}{a} = \frac{2\partial_{12}^2 V(0, 0)}{\partial_{11}^2 V(0, 0) + \partial_{22}^2 V(0, 0)}. \quad (3.4)$$

It is easy to see from site energy property (iv) that $a \neq 0$ so that η is well-defined.

The η term represents the relative strength of the long-range forces within the crystal against its stability. The effective strength of the long-range forces is represented by the numerator while the denominator represents its stability. In order for λ to be real valued, η can take only values between $[-1, 1]$. Outside of this range, the strength of the long-range forces overcomes the stability of the crystal and the ground state becomes unstable. For $|\eta| \geq 1$, site energy property (iv), the property enforcing stability, no longer holds as was shown in Theorem 2.1.2. Therefore, we restrict our attention of η to within the appropriate range for which $\lambda \in (-1, 1)$. In this range, η and λ have the opposite sign. The sign of η is in turn governed by the sign of the long-range interaction term b since the assumptions on the stability of the crystal imply that the denominator of η is always positive. The sign of b , therefore, has a significant effect on the qualitative behavior of the ground state. To see how this arises due to the interactions in the system, we can consider the linearized energy for the atomistic system about the Cauchy–Born ground state:

$$\mathcal{E}_{\text{lin}}^a(u) := \langle \delta \mathcal{E}^a(0), u' \rangle + \frac{1}{2} \langle \delta^2 \mathcal{E}^a(0) u', u' \rangle,$$

where we ignore any irrelevant constant terms. Using the identity

$$|u''_\ell|^2 := |u'_{\ell+1} - u'_\ell|^2 = |u'_{\ell+1}|^2 - 2u'_{\ell+1}u'_\ell + |u'_\ell|^2,$$

we may write the linearized energy in the following form:

$$\mathcal{E}_{\text{lin}}^a(u) = \partial_F V^{\text{surf}}(0)u'_0 + (a_s - a - b)|u'_0|^2 + \sum_{\ell=0}^{\infty} [(a + 2b)|u'_\ell|^2 - b|u''_\ell|^2],$$

where we have again used the constants from Eq. (2.16). The $-b|u''_\ell|^2$ term represents a significant portion of the long-range forces' influence in the system. When $b > 0$,

the system favors rapid fluctuations in the strain. In this regime, $\lambda < 0$ so that the alternating behavior in the strain is observed. When $b < 0$, this behavior is no longer energetically favorable and is suppressed.

We now wish to rewrite $(u^a)'_0$ into an alternative form that will be useful later. To do so, we first note that $W(F)$ achieves its minimum at $F = 0$. Therefore, we have the equality $-\partial_F V^{\text{surf}}(0) = -\partial_F \gamma(0)$ which we will use to change the numerator of $(u^a)'_0$. For the denominator, we simply use the definition of the constants a_s and b along with an explicit computation of $\partial_F^2 W(0)$ to find that

$$(u^a)'_0 = \frac{-\partial_F \gamma(0)}{\partial_F^2 W(0) + \partial_F^2 \gamma(0) + b(\lambda - 1)}.$$

In this form, it is clear that the strain at the surface in the linearized atomistic solution is similar to the initial strain found in the linearized surface Cauchy–Born model as shown in Eq. (3.3). The atomistic solution though includes a long-range force term represented by b that is absent in the surface Cauchy–Born solution.

The strains in the ground states for the linearized atomistic and surface Cauchy–Born systems with the EAM energy described in section 2.1.1 are shown in Figure (3.1). Note that the parameter λ here is negative, leading to an oscillatory behavior in the strain. Such qualitative behavior is expected as the system is meant to model the behavior of copper, which exhibits a similar oscillatory decay in the strain at its surface.

We now consider the parameter regime of η in which the surface Cauchy–Born approximation of the atomistic system is most accurate. Since the linearized surface Cauchy–Born solution only corrected the strain near the surface of the chain, the surface Cauchy–Born method should be most accurate when the surface effects are primarily concentrated at the surface in the atomistic system. As λ dictates the decay rate of the surface effects, the surface effects will become increasingly concentrated at the surface when $\lambda \rightarrow 0$. It is easy to see from the definition of λ that λ is close to 0 when $|\eta| \ll 1$. For such values of η , the long-range interactions in the crystal are weak relative to the stability of the crystal. In the limit as the long-range interactions weaken, the ground state should more closely resemble the homogeneous ground state of the Cauchy–Born solution, so the Cauchy–Born model should be most accurate in this regime as well. As $|\eta| \rightarrow 1$, however, the effects of the long-range interactions are of similar magnitude to

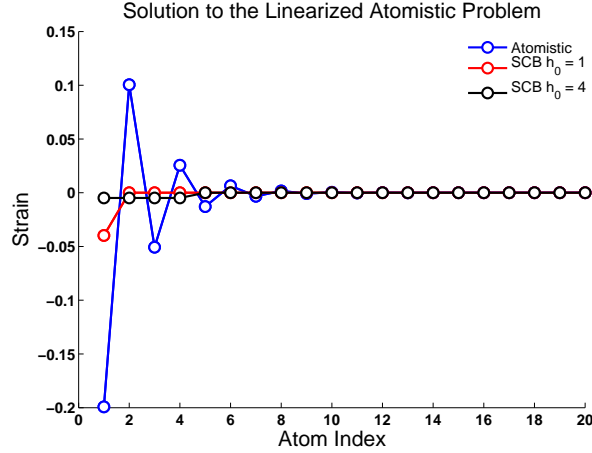


Figure 3.1: Computed ground states according to the linearized atomistic and the discretized surface Cauchy–Born method for two different surface element sizes.

the stability of the crystal. In this limit, $|\lambda| \rightarrow 1$, so surface effects will be felt far into the material. The surface Cauchy–Born method will clearly not be as accurate in this limit. Thus, the surface Cauchy–Born method should be most accurate when $|\eta| \ll 1$. We now consider a realistic system to see in which regime it falls.

3.1.1 Projected 3D Model

As the accuracy of the linearized surface Cauchy–Born model is dependent upon the parameter η , it would be useful to know in which regime this parameter falls for a realistic system. Thus, we will consider a planar surface relaxation model of a semi-infinite face-centered cubic (FCC) lattice whose constituents interact via a nearest-neighbor embedded atom model potential using parameters appropriate for copper [41] to compute η for a realistic problem. We will consider such a system by projecting the problem into 1-dimension so that we may make use of the analysis given above.

Let

$$\Lambda^{\text{FCC}} := \left\{ \xi = \sum_{i=1}^3 \mu_i \nu_i : \mu_1, \mu_2, \mu_3 \in \mathbb{Z} \right\}$$

denote the set of atomic positions within an FCC lattice with primitive lattice vectors

$$\nu_1 = \frac{1}{2}(0, 1, 1), \quad \nu_2 = \frac{1}{2}(1, 0, 1), \quad \nu_3 = \frac{1}{2}(1, 1, 0).$$

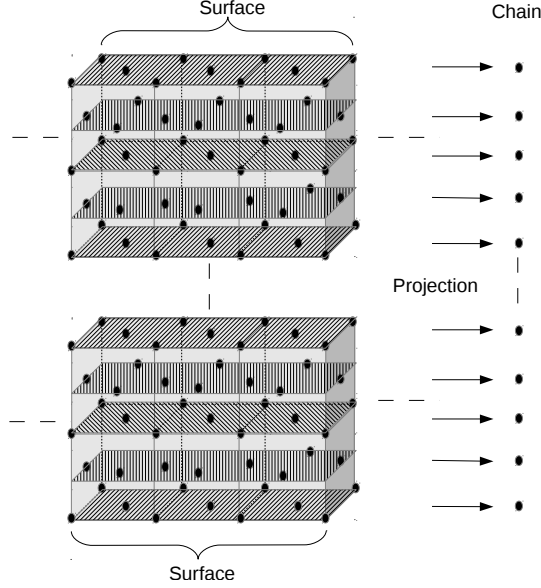


Figure 3.2: Visualization of the projection of $(0, 0, 1)$ planes of atoms into a 1D chain of atoms.

The cubic supercells are then generated by

$$(1, 0, 0) = -\nu_1 + \nu_2 + \nu_3 \quad (3.5)$$

$$(0, 1, 0) = \nu_1 - \nu_2 + \nu_3 \quad (3.6)$$

$$(0, 0, 1) = \nu_1 + \nu_2 - \nu_3. \quad (3.7)$$

We will consider a semi-infinite crystal slab whose atoms are located at the following positions:

$$\Lambda_{\text{slab}}^{\text{FCC}} := \{\xi \in \Lambda^{\text{FCC}} : \xi \cdot (1, 0, 0) \geq 0\}.$$

The atoms in the slab will be partitioned into planes which all have as their normal vector $(0, 0, 1)$. We restrict the movement of these planes of atoms to directions normal to their surface while holding the atoms' relative positions within the plane fixed. This restriction reduces the 3D surface relaxation problem to a 1D problem akin to the semi-infinite chain problem studied above. We will denote the energy per atom in a plane using a similar atomistic energy formulation from section 2.1.1 with a modification to

account for the fact that our atoms now have 12 nearest neighbors. We will let the planes in our system be indexed by the non-negative integers, and the displacement of these planes will be denoted by u_ℓ , $\ell \in \mathbb{Z}_{\geq 0}$. We define this energy per atom as

$$E_{\text{FCC}}^{\text{a}}(u) := 4\phi(0) + 4\phi(u'_0) + \psi(4\rho(0) + 4\rho(u'_0)) \\ + \sum_{\ell=0}^{\infty} \left[4\phi(0) + 4\phi(u'_\ell) + \psi(4\rho(0) + 4\rho(u'_{\ell-1}) + 4\rho(u'_{\ell+1})) \right],$$

where we again absorb the initial interatomic distance of 1 into the potentials and define $u'_\ell := u_{\ell+1} - u_\ell$. Note that our formulations of the potentials must also take into account the fact that the distance between the atoms in neighboring planes is not simply the distance between the planes.

Performing a similar analysis as was done for the linearized 1D model, we find that the strain in the ground state of our system decays exponentially with a base λ_{P3D} that is dependent upon the parameter η_{P3D} . The parameter η_{P3D} for this projected model is

$$\eta_{P3D} = \frac{16\psi''(12\rho(0))\rho'^2(0)}{4\phi''(0) + 8\psi'(12\rho(0))\rho''(0) + 32\psi''(12\rho(0))\rho'^2(0)}.$$

For the parameter values given in [41] for copper, we find that $\eta_{P3D} = 0.2546$. For this value of η_{P3D} , the surface relaxation will be oscillatory in addition to exponentially decaying into the material as is expected for metals. This value of η_{P3D} can be considered to be in the small parameter regime where the surface Cauchy–Born method is most accurate. Consequently, we are justified in analyzing the surface Cauchy–Born method for small values of η . We will now continue our examination of the error in the strain made by the surface Cauchy–Born method for the linearized 1D semi-infinite chain problem.

3.2 Asymptotic Analysis

Assuming that $|\eta| \ll 1$, we may perform an asymptotic analysis of the strain in the ground states for the linearized surface Cauchy–Born and atomistic models over the

first elements of their strain. We consider the limiting case when $a \rightarrow \infty$. Observe that

$$\eta = \frac{2b}{a} = \frac{2b}{\partial_F^2 W(0) - 2b}.$$

Thus, we may make the substitution $\partial_F^2 W(0) = 2b(1 + \frac{1}{\eta})$ in the linearized solutions to the ground state of the atomistic and surface Cauchy–Born systems.

Proposition 3.2.1. *Asymptotically, as $\eta \rightarrow 0$, we have that*

$$\begin{aligned} (U^{\text{scb}})'_0 &= -\partial_F \gamma(0) \left[\frac{\eta}{2h_0 b} - (\partial_F^2 \gamma(0) + 2h_0 b) \left(\frac{\eta}{2h_0 b} \right)^2 + \mathcal{O}(\eta^3) \right] \\ (u^{\text{a}})'_0 &= -\partial_F \gamma(0) \left[\frac{\eta}{2b} - (\partial_F^2 \gamma(0) + b) \left(\frac{\eta}{2b} \right)^2 + \mathcal{O}(\eta^3) \right]. \end{aligned}$$

Proof. Omitted. □

3.2.1 Strain Relative Error Analysis

To investigate the strain error made by the surface Cauchy–Born method in comparison with the bulk Cauchy–Born method, we will first interpolate the displacement gradients found using the finite-element approximation of these two methods. We will do so by defining

$$u'_\ell := U'_j, \text{ for } \ell = X_j, X_j + 1, \dots, X_{j+1} - 1, \text{ for all } j \in \mathbb{Z}_{\geq 0}$$

for both the surface and bulk Cauchy–Born methods.

We are interested in investigating the relative error between the linearized surface Cauchy–Born and bulk Cauchy–Born methods. Let $p \in [1, \infty]$. We will consider the relative error defined by

$$\text{Err}_p := \frac{\|(u^{\text{a}})' - (u^{\text{scb}})'\|_{\ell^p}}{\|(u^{\text{a}})' - (u^{\text{cb}})'\|_{\ell^p}} = \frac{\|(u^{\text{a}})' - (u^{\text{scb}})'\|_{\ell^p}}{\|(u^{\text{a}})'\|_{\ell^p}}.$$

The rate of convergence of the relative error will depend upon the size of the first element h_0 , which should be evident from our formulas for the surface displacement gradients in the atomistic and surface Cauchy–Born linearized models. This difference in convergence is a result of the finite element approximation of the surface Cauchy–Born model.

Proposition 3.2.2 (Strain Error). *Let $p \in [1, \infty]$ and $h_0 > 1$, then*

$$Err_p = C_p + \mathcal{O}(\eta),$$

where $\frac{1}{2} \leq C_p \leq 2$. If $h_0 = 1$, then

$$Err_p = 2^{1/p}|\eta| + \mathcal{O}(\eta^2).$$

Proof. We will first consider the case when $h_0 = 1$ for $p \in [1, \infty)$. The denominator of the relative strain error is given by

$$\|(u^a)'\|_{\ell^p} = \left(\sum_{\ell=0}^{\infty} |(u^a)'_{\ell}|^p \right)^{1/p} = \frac{|(u^a)'_0|}{(1 - \lambda^p)^{1/p}}.$$

In the limit as $\eta \rightarrow 0$, we may use Eq. (3.4) to show that

$$\lambda = -\frac{\eta}{2} - \frac{\eta^3}{8} + \mathcal{O}(\eta^5). \quad (3.8)$$

Therefore, we have that

$$\frac{1}{(1 - \lambda^p)^{1/p}} = 1 + \mathcal{O}(\lambda^p) = 1 + \mathcal{O}(\eta^p).$$

Multiplying this result with our asymptotic expansion of $(u^a)'_0$ from Proposition 3.2.1 gives us that

$$\|(u^a)'\|_{\ell^p} = \left| \frac{\partial_F \gamma(0)}{4b} \eta \right| + \mathcal{O}(\eta^2).$$

Now, we consider the numerator. Using a similar approach as above, we find that

$$\left(\sum_{\ell=1}^{\infty} |(u^a)'_{\ell}|^p \right)^{1/p} = \frac{|(u^a)'_0| |\lambda|}{(1 - \lambda^p)^{1/p}} = \left| \frac{\partial_F \gamma(0)}{4b} \eta^2 \right| + \mathcal{O}(\eta^3).$$

For the first bond, we take the difference of the asymptotic expansions as stated in

Proposition 3.2.1:

$$\begin{aligned} |(u^a)'_0 - (u^{\text{scb}})'_0| &= |\partial_F \gamma(0)| \left| \frac{\eta}{2b} \left(1 - \frac{1}{h_0}\right) \right. \\ &\quad \left. - \frac{\eta^2}{2b^2} \left[b \left(1 - \frac{2}{h_0}\right) + \partial_F^2 \gamma(0) \left(1 - \frac{1}{h_0^2}\right) \right] \right| + \mathcal{O}(\eta^3) \\ &= \left| \frac{\partial_F \gamma(0)}{4b} \eta^2 \right| + \mathcal{O}(\eta^3). \end{aligned}$$

Therefore,

$$\|(u^a)' - (u^{\text{scb}})'\|_{\ell^p} = 2^{1/p} \left| \frac{\partial_F \gamma(0)}{4b} \eta^2 \right| + \mathcal{O}(\eta^3).$$

The relative error in the case of $h_0 = 1$ is

$$\text{Err}_p = \frac{2^{1/p} \left| \frac{\partial_F \gamma(0)}{4b} \right| |\eta|^2 + \mathcal{O}(\eta^3)}{\left| \frac{\partial_F \gamma(0)}{4b} \right| |\eta| + \mathcal{O}(\eta^2)} = 2^{1/p} |\eta| + \mathcal{O}(\eta^2).$$

This concludes the proof for the convergence when $h_0 = 1$.

When we have $h_0 > 1$ for $p \in [1, \infty)$, we do not have the cancellation in lower order terms over the first bond. The error in the numerator of the relative error will now be

$$\|(u^a)' - (u^{\text{scb}})'\|_{\ell^p} = |\eta| \left| \frac{\partial_F \gamma(0)}{2b} \right| \left(\left| 1 - \frac{1}{h_0} \right|^p + \sum_{\ell=1}^{X_1-1} \left| \frac{1}{h_0} \right|^p \right)^{1/p} + \mathcal{O}(\eta^2).$$

As the denominator is unchanged for a larger first element in the Cauchy–Born approximations, the above result implies the convergence of the relative error for $h_0 > 1$ is as stated in the proposition. The proof for the $p = \infty$ case is similar to that given above, so we will not present it here. \square

The above result indicates that the surface Cauchy–Born method is actually less accurate than the bulk Cauchy–Born method with regard to certain ℓ^p norms when we employ a coarse mesh at the boundary. By taking an atomistic spacing at the boundary layer though, the relative error converges linearly to 0 in terms of η . As we are considering the regime in which η is small, this implies that the surface Cauchy–Born has a smaller error than the bulk Cauchy–Born approximation in all norms when

we use atomistic spacing at the boundary. A log-log plot demonstrating the rates of convergence shown above for the ℓ_2 relative strain error is provided in Figure 3.3.

The previous relative norm represents the pointwise accuracy of the Cauchy–Born approximations. Often, knowing just the mean strain is useful, so we now consider a relative mean strain error defined by

$$\overline{Err} := \left| \frac{\sum_{\ell=0}^{\infty} ((u^a)'_{\ell} - (u^{\text{scb}})'_{\ell})}{\sum_{\ell=0}^{\infty} ((u^a)'_{\ell} - (u^{\text{cb}})'_{\ell})} \right| = \left| \frac{\sum_{\ell=0}^{\infty} ((u^a)'_{\ell} - (u^{\text{scb}})'_{\ell})}{\sum_{\ell=0}^{\infty} (u^a)'_{\ell}} \right|.$$

Proposition 3.2.3 (Mean Strain Error). *Let $h_0 > 0$. Then,*

$$\overline{Err} = \left| \frac{\partial_F^2 \gamma(0)}{2b} \right| \left(1 - \frac{1}{h_0} \right) |\eta| + \mathcal{O}(\eta^2).$$

Proof. To begin the proof, we observe that

$$\sum_{\ell=0}^{\infty} (u^a)'_{\ell} = \frac{(u^a)'_0}{1 - \lambda}.$$

Using the asymptotic expansion for η gives us

$$\frac{1}{1 - \lambda} = 1 + \lambda + \lambda^2 + \mathcal{O}(\lambda^3) = 1 - \frac{\eta}{2} + \frac{\eta^2}{4} + \mathcal{O}(\eta^3).$$

Therefore,

$$\sum_{\ell=0}^{\infty} (u^a)'_{\ell} = -\partial_F \gamma(0) \left[\frac{\eta}{2b} - \left(\frac{\eta}{2b} \right)^2 (\partial_F^2 \gamma(0) + 2b) \right] + \mathcal{O}(\eta^3).$$

The SCB term is easier to compute. It is simply

$$\sum_{\ell=0}^{\infty} (u^{\text{scb}})'_{\ell} = h_0 (U^{\text{scb}})'_0 = -\partial_F \gamma(0) \left[\frac{\eta}{2b} - \left(\frac{\eta}{2b} \right)^2 \left(\frac{\partial_F \gamma(0)}{h_0} + 2b \right) \right] + \mathcal{O}(\eta^3).$$

Now, subtract the mean atomistic and surface Cauchy–Born strains:

$$\sum_{\ell=0}^{\infty} \left((u^a)'_{\ell} - (u^{\text{scb}})'_{\ell} \right) = \partial_F \gamma(0) \partial_F^2 \gamma(0) \left(1 - \frac{1}{h_0} \right) \left(\frac{\eta}{2b} \right)^2 + \mathcal{O}(\eta^3).$$

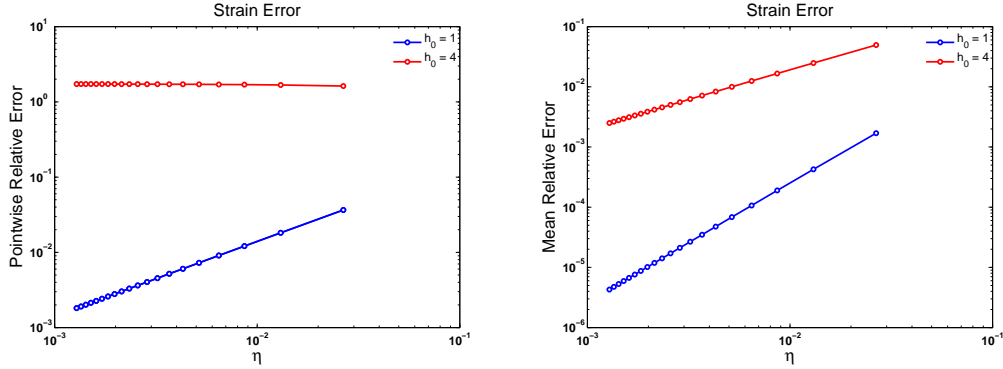


Figure 3.3: ℓ_2 Pointwise and Mean Relative Error Decay Rates

Dividing this difference by the mean atomistic strain yields the stated result. \square

The mean strain error converges to 0 as $\eta \rightarrow 0$ an order of magnitude faster than the pointwise error. This behavior has been observed even in applications of the method in higher dimension such as in [17]. A log-log plot demonstrating this rate of convergence for the mean strain error is provided in Figure 3.3.

This concludes the analysis for the surface Cauchy–Born method in 1D. While the analysis is simple, it is instructive in highlighting the advantages and difficulties of the method. In particular, the surface Cauchy–Born method does represent an improvement over the regular Cauchy–Born method when the surface element has atomistic spacing. However, there is little control over the error once this choice is made. In the next chapter, we develop an alternative approach to capturing surface effects that offers greater control over the quality of the surface model’s approximation.

Remark. The analysis performed in this section may also be performed for a system with a finite number of atoms. The results translate almost verbatim with the only addition being an identical surface effect term arising at the other end of the chain. In particular, the parameter η for the finite case is the same as for the semi-infinite case and the physical interpretation of this parameter used above works in the finite case as well. In addition, these results hold for next-nearest neighbor interaction models like those discussed in [38].

Chapter 4

Predictor-Corrector Method

4.1 Corrector Model

Proposition 2.2.1 demonstrates that the Cauchy–Born method alone is incapable of accurately approximating the behavior of atomistic systems with surfaces due to an inconsistency in the forces at the surface. However, the Cauchy–Born method is an excellent method for approximating the bulk response of materials and Theorem 2.1.2 indicates that the error due to surface effects may be quite localized. Hence, in this section, we propose a predictor-corrector method for accurately and efficiently approximating the atomistic surface problem with the initial prediction for material behavior provided by the Cauchy–Born model. A separate correction to the Cauchy–Born solution on a boundary layer at the surface of the chain will then be applied to take into account surface effects. The initial Cauchy–Born solution plus these corrections form the predictor-corrector method’s approximation of the minimizer of the semi-infinite chain under dead-load forces. In symbols, we hope to be able to compute a corrector strain q_L so that we have the following approximation:

$$u^a \approx \Pi_a u^{\text{cb}} + q_L, \tag{4.1}$$

where u^a is the solution to the atomistic problem (2.5) and u^{cb} is the solution to the Cauchy–Born problem (2.24). The size of the boundary layer in the corrector method will be a controllable parameter, and its adjustment will allow for a systematic control

over the accuracy of the approximation. Proving the validity of the decomposition of the atomistic minimizer into a bulk response and a surface correction will be the primary goal in the analysis of the method.

Given a predictor u^{cb} solving the Cauchy–Born problem (2.24), we define the corrector problem via the minimization of a corrector energy, which is given by

$$\begin{aligned} \mathcal{E}^\Gamma(q; F_0) &= V^{\text{surf}}(F_0 + q'_0) - W(F_0) - q'_0 \partial_F W(F_0) \\ &+ \sum_{j=1}^{\infty} (V(F_0 + q'_{j-1}, F_0 + q'_j) - W(F_0) - q'_j \partial_F W(F_0)), \end{aligned} \quad (4.2)$$

where we will normally take $F_0 := \nabla u^{\text{cb}}(0)$.

The idea of the corrector problem is that it should depend only in a local way on the elastic field ∇u^{cb} . In this case, this dependence is only on $\nabla u^{\text{cb}}(0)$. This choice was made deliberately so that the corrector problem can be understood as a cell problem on a surface element when the Cauchy–Born model is discretized using finite elements.

The major difference between solving the corrector problem versus the fully atomistic problem is the space in which we seek our minimizer. The corrector strain is found by solving the following minimization problem:

$$q_L \in \arg \min \{ \mathcal{E}^\Gamma(q; u^{\text{cb}}) \mid q \in \mathcal{Q}_L \}, \quad (4.3)$$

where \mathcal{Q}_L is the boundary layer over which we correct the Cauchy–Born solution and $L \in \mathbb{N} \cup \{\infty\}$ is the size of the boundary layer. When $L \in \mathbb{N}$,

$$\mathcal{Q}_L := \{q \in \mathcal{U} \mid q_\ell = 0 \text{ for all } \ell \geq L\}.$$

For $L = \infty$, we simply have that

$$\mathcal{Q}_\infty := \mathcal{U}.$$

The size of L will affect both the computational expense necessary to solve the corrector problem and the final accuracy of the predictor-corrector method's approximation of the atomistic system's behavior. Increasing L increases the computational expense and increases the accuracy of the approximation. However, as we expect surface effects to be extremely localized, it should be possible to use a boundary layer much smaller than

the entire domain in order to obtain a reasonably accurate yet less computationally intensive solution. Note that the external force f does not enter directly into the corrector problem. The Cauchy–Born method accounts for the external forces on its own, but the influence of the external force is felt through the F_0 term. For small enough f , the existence of a solution to the corrector problem in the case of the infinite boundary layer can be proven.

Theorem 4.1.1. *There exists $\varepsilon_\Gamma > 0$ such that, for all $F_0 \in \mathbb{R}$ with $|F_0| < \varepsilon_\Gamma$, the corrector problem (4.3) with $L = \infty$ has a solution $q_\infty \in \mathcal{Q}_\infty$. For all $v \in \mathcal{Q}_\infty$, this solution q_∞ satisfies*

$$\langle \delta^2 \mathcal{E}^\Gamma(q_\infty; F_0)v, v \rangle \geq \frac{c_a}{2} \|v'\|_{\ell^2}^2, \quad (4.4)$$

where c_a is the atomistic stability constant for u_{gr}^a in (2.21). In addition, there exists a constant $0 \leq \mu_q < 1$ such that

$$|(q_\infty)'_\ell| \lesssim \mu_q^\ell \quad \text{for all } \ell \in \mathbb{Z}_{\geq 0}. \quad (4.5)$$

Proof. Since the corrector method requires a Cauchy–Born solution, we first suppose that f is small enough such that Theorem 2.2.3 applies. The quantitative inverse function theorem, or Theorem A.2.1, will be used to prove the existence of the corrector solution and its stability for sufficiently small external forces. The inverse function theorem requires that we derive consistency and stability estimates for the corrector energy, which we will now show.

Consistency: It is reasonable to expect that, for $|F_0|$ small, the corrector solution q_∞ be close to u_{gr}^a since the corrector energy simply becomes the atomistic energy. Therefore, we may find q_∞ by applying the inverse function theorem in a neighborhood of u_{gr}^a . From Proposition A.1.1, the first variation of the corrector energy evaluated at $\tilde{q} = u_{\text{gr}}^a$ is

$$\begin{aligned} \langle \delta \mathcal{E}^\Gamma(\tilde{q}; F_0), v \rangle &= v'_0 \left\{ \partial_F V^{\text{surf}}(F_0 + \tilde{q}'_0) + \partial_1 V(F_0 + \tilde{q}'_0, F_0 + \tilde{q}'_1) - \partial_F W(F_0) \right\} \\ &+ \sum_{\ell=1}^{\infty} v'_\ell \left\{ \partial_2 V(F_0 + \tilde{q}'_{\ell-1}, F_0 + \tilde{q}'_\ell) + \partial_1 V(F_0 + \tilde{q}'_\ell, F_0 + \tilde{q}'_{\ell+1}) - \partial_F W(F_0) \right\}, \end{aligned}$$

where $v \in \mathcal{Q}_\infty$. Using the fact that $\delta\mathcal{E}^a(\tilde{q}) = 0$ and $\partial_F W(0) = 0$, we obtain

$$\begin{aligned}
\langle \delta\mathcal{E}^\Gamma(\tilde{q}; F_0), v \rangle &= \langle \delta\mathcal{E}^\Gamma(\tilde{q}; F_0) - \delta\mathcal{E}^a(\tilde{q}), v \rangle \\
&= v'_0 \left\{ \partial_F V^{\text{surf}}(F_0 + \tilde{q}'_0) + \partial_1 V(F_0 + \tilde{q}'_0, F_0 + \tilde{q}'_1) - \partial_F W(F_0) \right. \\
&\quad \left. - \partial_F V^{\text{surf}}(\tilde{q}'_0) - \partial_1 V(\tilde{q}'_0, \tilde{q}'_1) + \partial_F W(0) \right\} \\
&\quad + \sum_{\ell=1}^{\infty} v'_\ell \left\{ \partial_2 V(F_0 + \tilde{q}'_{\ell-1}, F_0 + \tilde{q}'_\ell) + \partial_1 V(F_0 + \tilde{q}'_\ell, F_0 + \tilde{q}'_{\ell+1}) - \partial_F W(F_0) \right. \\
&\quad \left. - \partial_2 V(\tilde{q}'_{\ell-1}, \tilde{q}'_\ell) - \partial_1 V(\tilde{q}'_\ell, \tilde{q}'_{\ell+1}) + \partial_F W(0) \right\} \\
&=: \sum_{\ell=0}^{\infty} v'_\ell A_\ell.
\end{aligned}$$

From the Lipschitz continuity of the site energies, we see that

$$|A_0| \lesssim |F_0|.$$

To estimate A_ℓ for $\ell \geq 1$, we proceed more carefully. Expanding with respect to \tilde{q}_j for $j = \ell - 1, \ell, \ell + 1$, employing the identity $\partial_F W(F) = \partial_1 V(F, F) + \partial_2 V(F, F)$, and finally making use of the global Lipschitz continuity of $\partial^2 V$ yields

$$\begin{aligned}
|A_\ell| &= \left| \left\{ \partial_2 V(F_0, F_0) + \partial_1 V(F_0, F_0) - \partial_F W(F_0) \right\} - \left\{ \partial_2 V(0, 0) + \partial_1 V(0, 0) - \partial_F W(0) \right\} \right. \\
&\quad + \int_0^1 \left\{ \partial \partial_2 V(F_0 + t\tilde{q}'_{\ell-1}, F_0 + t\tilde{q}'_\ell) - \partial \partial_2 V(t\tilde{q}'_{\ell-1}, t\tilde{q}'_\ell) \right\} \cdot \begin{pmatrix} \tilde{q}'_{\ell-1} \\ \tilde{q}'_\ell \end{pmatrix} dt \\
&\quad \left. + \int_0^1 \left\{ \partial \partial_1 V(F_0 + t\tilde{q}'_\ell, F_0 + t\tilde{q}'_{\ell+1}) - \partial \partial_1 V(t\tilde{q}'_\ell, t\tilde{q}'_{\ell+1}) \right\} \cdot \begin{pmatrix} \tilde{q}'_\ell \\ \tilde{q}'_{\ell+1} \end{pmatrix} dt \right| \\
&\lesssim |F_0| (|\tilde{q}'_{\ell-1}| + |\tilde{q}'_\ell| + |\tilde{q}'_{\ell+1}|).
\end{aligned}$$

With the now derived bounds on all of the A_ℓ , we may use the Cauchy-Schwarz inequality to show that

$$\langle \delta\mathcal{E}^\Gamma(\tilde{q}; F_0), v \rangle \leq \|A\|_{\ell^2} \|v'\|_{\ell^2} \lesssim |F_0| (1 + \|\tilde{q}'\|_{\ell^2}) \|v'\|_{\ell^2}. \quad (4.6)$$

The magnitude of the residual may be controlled through the $|F_0|$ term.

Stability: Recall that $\tilde{q} = u_{\text{gr}}^a$ is strongly stable in the atomistic model (2.21) with stability constant $c_a > 0$. To prove the stability of $\delta^2 \mathcal{E}^\Gamma(\tilde{q}; F_0)$, we will simply bound the error in the Hessians. The second variation in the atomistic energy from Proposition A.1.2 may be rewritten in the following way:

$$\begin{aligned} \langle \delta^2 \mathcal{E}^a(u)v, v \rangle &= |v'_0|^2 \left\{ \partial_F^2 V^{\text{surf}}(u'_0) \right\} + \sum_{\ell=0}^{\infty} \left[|v'_\ell + v'_{\ell+1}|^2 \left\{ \partial_{12}^2 V(u'_\ell, u'_{\ell+1}) \right\} \right. \\ &\quad + |v'_\ell|^2 \left\{ \partial_{11}^2 V(u'_\ell, u'_{\ell+1}) - \partial_{12}^2 V(u'_\ell, u'_{\ell+1}) \right\} \\ &\quad \left. + |v'_{\ell+1}|^2 \left\{ \partial_{22}^2 V(u'_\ell, u'_{\ell+1}) - \partial_{12}^2 V(u'_\ell, u'_{\ell+1}) \right\} \right]. \end{aligned}$$

We note that the second variation for the corrector energy has the same form as the second variation for the atomistic energy. Therefore, the difference between the Hessians is

$$\begin{aligned} \langle (\delta^2 \mathcal{E}^a(\tilde{q}) - \delta^2 \mathcal{E}^\Gamma(\tilde{q}; F_0))v, v \rangle &= |v'_0|^2 \left\{ \partial_F^2 V^{\text{surf}}(\tilde{q}'_0) - \partial_F^2 V^{\text{surf}}(F_0 + \tilde{q}'_0) \right\} \\ &\quad + \sum_{\ell=0}^{\infty} \left[|v'_\ell + v'_{\ell+1}|^2 \left\{ \partial_{12}^2 V(\tilde{q}'_\ell, \tilde{q}'_{\ell+1}) - \partial_{12}^2 V(F_0 + \tilde{q}'_\ell, F_0 + \tilde{q}'_{\ell+1}) \right\} \right. \\ &\quad \quad + |v'_\ell|^2 \left\{ \partial_{11}^2 V(\tilde{q}'_\ell, \tilde{q}'_{\ell+1}) - \partial_{12}^2 V(\tilde{q}'_\ell, \tilde{q}'_{\ell+1}) \right. \\ &\quad \quad \left. - \partial_{11}^2 V(F_0 + \tilde{q}'_\ell, F_0 + \tilde{q}'_{\ell+1}) + \partial_{12}^2 V(F_0 + \tilde{q}'_\ell, F_0 + \tilde{q}'_{\ell+1}) \right\} \\ &\quad \quad + |v'_{\ell+1}|^2 \left\{ \partial_{22}^2 V(\tilde{q}'_\ell, \tilde{q}'_{\ell+1}) - \partial_{12}^2 V(\tilde{q}'_\ell, \tilde{q}'_{\ell+1}) \right. \\ &\quad \quad \left. - \partial_{22}^2 V(F_0 + \tilde{q}'_\ell, F_0 + \tilde{q}'_{\ell+1}) + \partial_{12}^2 V(F_0 + \tilde{q}'_\ell, F_0 + \tilde{q}'_{\ell+1}) \right\} \left. \right]. \end{aligned}$$

The Lipschitz continuity of $\partial_F^2 V^{\text{surf}}$ and $\partial^2 V$ can be used to provide a bound in terms of $|F_0|$:

$$|\langle (\delta^2 \mathcal{E}^a(\tilde{q}) - \delta^2 \mathcal{E}^\Gamma(\tilde{q}; F_0))v, v \rangle| \leq C|F_0| \|v'\|_{\ell^2}^2,$$

where the constant C is the upper bound on the Lipschitz constants involved in the estimate multiplied by a simple factor. Thus, we obtain, for $|F_0| \leq \frac{1}{4}c_a/C$, that

$$\langle \delta^2 \mathcal{E}^\Gamma(\tilde{q}; F_0)v, v \rangle \geq \frac{3c_a}{4} \|v'\|_{\ell^2}^2 \quad \text{for all } v \in \mathcal{Q}_\infty. \quad (4.7)$$

The consistency estimate in (4.6), the stability estimate in (4.7), and the Lipschitz continuity of $q \mapsto \delta^2 \mathcal{E}^\Gamma(q; F_0)$ satisfy the assumptions of Theorem A.2.1 which then implies the existence of a minimizer q_∞ with $\|\tilde{q}' - q'_\infty\|_{\ell^2} \lesssim |F_0|$. Choosing F_0 sufficiently small implies the final inequality in (4.4).

The exponential decay in (4.5) follows from a simple modification of Theorem 2.1.2 since the atomistic and corrector energies are so similar. \square

In order to make the predictor-corrector method computationally reasonable, we wish to solve the corrector problem over a small boundary layer. This necessitates a cut-off operator that introduces an additional error to the problem. Therefore, it is necessary to introduce a projection operator from the space \mathcal{Q}_∞ to \mathcal{Q}_L . For some constant $L > 0$, we define the cut-off operator $\Pi_L : \mathcal{Q}_\infty \rightarrow \mathcal{Q}_L$ by how it modifies strains:

$$(\Pi_L q)_\ell' := \begin{cases} q'_\ell, & \ell = 0, \dots, L, \\ 0, & \ell > L. \end{cases}$$

We now prove the error that results from employing this cut-off operator on exponentially decaying solutions.

Lemma 4.1.2. *Let $q \in \mathcal{Q}_\infty$ satisfy $|q'_\ell| \lesssim \mu^\ell$ for some $\mu \in [0, 1)$ for all ℓ . Then,*

$$\|q' - \Pi_L q'\|_{\ell^2} \lesssim \mu^L.$$

Proof. First, note that

$$q'_\ell - (\Pi_L q)_\ell' = \begin{cases} 0, & 0 \leq \ell \leq L-1, \\ q'_\ell, & \ell > L. \end{cases}$$

Thus,

$$\|q' - \Pi_L q'\|_{\ell^2}^2 = \sum_{\ell=L}^{\infty} |q'_\ell|^2 \lesssim \sum_{\ell=L}^{\infty} \mu^{2\ell} = \frac{\mu^{2L}}{1 - \mu^2}.$$

Since μ is independent of L , we have the desired result. \square

We can now consider the existence of a solution to the corrector problem for a finite boundary layer as an approximation of the infinite case.

Proposition 4.1.3. *Under the conditions of Theorem 4.1.1, there exists $L_0 > 0$ such that the corrector problem (4.3) with $L \geq L_0$ has a solution $q_L \in \mathcal{Q}_L$ satisfying*

$$\|q'_\infty - q'_L\|_{\ell^2} \lesssim \mu_q^L.$$

Proof. Let q_∞ be the solution to the infinite corrector problem. The result is proven by an application of the quantitative inverse function theorem, Theorem A.2.1, using the projected solution $\Pi_L q_\infty$ as an approximate solution. Observe that

$$\langle \delta \mathcal{E}^\Gamma(q_\infty; F_0), v \rangle = 0 \quad \text{for all } v \in \mathcal{Q}_L \subset \mathcal{Q}_\infty$$

since q_∞ is a solution in a larger space. By the Lipschitz continuity of the first variation in the corrector energy,

$$|\langle \delta \mathcal{E}^\Gamma(\Pi_L q_\infty; F_0), v \rangle| = |\langle \delta \mathcal{E}^\Gamma(\Pi_L q_\infty; F_0) - \delta \mathcal{E}^\Gamma(q_\infty; F_0), v \rangle| \lesssim \|q'_\infty - \Pi_L q'_\infty\|_{\ell^2} \|v'\|_{\ell^2}.$$

According to Theorem 4.1.1, there exists $0 \leq \mu_q < 1$ such that $|(q_\infty)'_\ell| \lesssim \mu_q^\ell$. Hence, Lemma 4.1.2 may be applied to show that

$$\|\delta \mathcal{E}^\Gamma(\Pi_L q_\infty; F_0)\|_{\mathcal{Q}_L^*} = \sup_{v \in \mathcal{Q}_L, \|v'\|_{\ell^2}=1} |\langle \delta \mathcal{E}^\Gamma(\Pi_L q_\infty; F_0), v \rangle| \lesssim \mu_q^L. \quad (4.8)$$

For the stability of $\Pi_L q_\infty$, we can make use of the stability of q_∞ from Theorem 4.1.1, the result of Lemma 4.1.2, and the Lipschitz continuity of the second variation of the corrector energy to find that

$$\begin{aligned} \langle \delta \mathcal{E}^\Gamma(\Pi_L q_\infty; F_0)v, v \rangle &= \langle \delta \mathcal{E}^\Gamma(q_\infty; F_0)v, v \rangle - \left[\langle \delta \mathcal{E}^\Gamma(\Pi_L q_\infty; F_0)v, v \rangle - \langle \delta \mathcal{E}^\Gamma(q_\infty; F_0)v, v \rangle \right] \\ &\geq \langle \delta \mathcal{E}^\Gamma(q_\infty; F_0)v, v \rangle - M \|q'_\infty - \Pi_L q'_\infty\|_{\ell^2} \|v'\|_{\ell^2}^2 \\ &\geq \left(\frac{c_a}{2} - CM\mu_q^L \right) \|v'\|_{\ell^2}, \end{aligned}$$

where M is the Lipschitz constant for \mathcal{E}^Γ and C is the unlisted constant in (4.8).

For L sufficiently large, all assumptions of Theorem A.2.1 are met, and its application completes the proof. \square

4.2 Predictor-Corrector Approximation

If $\|f\|_{\mathcal{U}^*}$ is sufficiently small, then Theorem 2.2.3 guarantees the existence of a solution $u^{\text{cb}} \in \mathcal{U}^{\text{cb}}$ with $|\nabla u^{\text{cb}}(0)| \leq \varepsilon_\Gamma$. Thus, if we choose a sufficiently large boundary layer for the corrector problem (4.3), Theorem 4.1.1 and Proposition 4.1.3 ensure that the predictor-corrector approximation

$$u_L^{\text{pc}} := \Pi_a u^{\text{cb}} + q_L$$

is well-defined. In order to determine the accuracy of this approximation, we show that a solution to the atomistic problem (2.5) exists in a neighborhood of u_L^{pc} , which we quantify. We first state the result along with a brief remark before proving the essential components of the theorem.

Theorem 4.2.1. *There exists an $\varepsilon > 0$ such that, for all $f \in \mathcal{U}^*$ with $\|f\|_{\mathcal{U}^*} < \varepsilon$, there exists an atomistic solution $u^{\text{a}} \in \mathcal{U}$ to (2.5) satisfying*

$$\|(u^{\text{a}})' - (u_L^{\text{pc}})'\|_{\ell^2} \lesssim \mu_q^L + |\nabla^2 u^{\text{cb}}(0)| + \|\nabla^2 u^{\text{cb}}\|_{L^4}^2 + \|\nabla^3 u^{\text{cb}}\|_{L^2} + \|\nabla f\|_{L^2}. \quad (4.9)$$

Proof. This result is a consequence of the inverse function theorem (Theorem A.2.1) and Theorems 4.2.3 (Consistency) and 4.2.4 (Stability). \square

Remark. The term μ_q^L arises from the finite boundary layer approximation of the corrector problem. The term $|\nabla^2 u^{\text{cb}}(0)|$ stems from the substitution of the nonlinear elastic field $\nabla u^{\text{cb}}(x)$ in the corrector with the homogeneous strain $\nabla u^{\text{cb}}(0)$. This error is uncontrollable in the sense that it cannot be reduced with a numerical parameter. This motivates a potential choice for the size of the boundary layer as one can balance the error due to μ_q^L with the error from the $\nabla u^{\text{cb}}(0)$ term by choosing L to be proportional to the appropriate logarithm of $|\nabla^2 u^{\text{cb}}(0)|$. Finally, the $\|\nabla^2 u^{\text{cb}}\|_{L^4}^2 + \|\nabla^3 u^{\text{cb}}\|_{L^2}$ term is the usual Cauchy–Born modeling error, and the $\|\nabla f\|_{L^2}$ term represents the error made in the continuum approximation of the applied forces.

Now, we prove the necessary consistency error estimate in the next two theorems. We make use of the following notation in the following statements and proofs:

$$u_\ell'' := u'_{\ell+1} - u'_\ell \quad \text{and} \quad u_\ell''' := u'_{\ell-1} - 2u'_\ell + u'_\ell.$$

Theorem 4.2.2. *Let $w, q \in \mathcal{U}$, $u := w + q$, and $F_0 := w'_0$. Then, for all $v \in \mathcal{U}$,*

$$\begin{aligned} |\langle \delta\mathcal{E}^a(u) - \delta\mathcal{E}^{\text{cb}}(w) - \delta\mathcal{E}^\Gamma(q; F_0), v \rangle| &\lesssim \left[\|w''\|_{\ell^4(\mathbb{Z}_{\geq 0})}^2 + \|w'''\|_{\ell^2(\mathbb{Z}_{> 0})} + \|q'' \cdot w''\|_{\ell^2(\mathbb{Z}_{\geq 0})} \right. \\ &\quad \left. + |w'_1 - F_0| + \left(\sum_{\ell=1}^{\infty} (|q'_{\ell-1}| + |q'_\ell| + |q'_{\ell+1}|)^2 |w'_\ell - F_0|^2 \right)^{1/2} \right] \cdot \|v\|_{\ell^2}. \end{aligned}$$

Proof. The difference in the first variations is given by

$$\begin{aligned} &\langle \delta\mathcal{E}^a(u) - \delta\mathcal{E}^{\text{cb}}(w) - \delta\mathcal{E}^\Gamma(q; F_0), v \rangle \\ &= v'_0 \left[\left\{ \partial_F V^{\text{surf}}(u'_0) + \partial_1 V(u'_0, u'_1) \right\} - \left\{ \partial_F W(F_0) \right\} \right. \\ &\quad \left. - \left\{ \partial_F V^{\text{surf}}(F_0 + q'_0) + \partial_1 V(F_0 + q'_0, F_0 + q'_1) - \partial_F W(F_0) \right\} \right] \\ &\quad + \sum_{\ell=1}^{\infty} v'_\ell \left[\left\{ \partial_2 V(u'_{\ell-1}, u'_\ell) + \partial_1 V(u'_\ell, u'_{\ell+1}) \right\} - \left\{ \partial_F W(w'_\ell) \right\} \right. \\ &\quad \left. - \left\{ \partial_2 V(F_0 + q'_{\ell-1}, F_0 + q'_\ell) + \partial_1 V(F_0 + q'_\ell, F_0 + q'_{\ell+1}) - \partial_F W(F_0) \right\} \right] \\ &=: S + B, \end{aligned}$$

where S, B denote, respectively, the surface and bulk contributions to the consistency error.

Surface term: Using the Lipschitz continuity of the bulk site energy, we can show

that

$$\begin{aligned}
|S| &= \left| v'_0 \left[\left\{ \partial_F V^{\text{surf}}(u'_0) + \partial_1 V(u'_0, u'_1) \right\} - \left\{ \partial_F W(F_0) \right\} \right. \right. \\
&\quad \left. \left. - \left\{ \partial_F V^{\text{surf}}(F_0 + q'_0) + \partial_1 V(F_0 + q'_0, F_0 + q'_1) - \partial_F W(F_0) \right\} \right] \right| \\
&= |v'_0| \left| \partial_1 V(F_0 + q'_0, w'_1 + q'_1) - \partial_1 V(F_0 + q'_0, F_0 + q'_1) \right| \\
&\lesssim |v'_0| \cdot |w'_1 - F_0|, \tag{4.10}
\end{aligned}$$

where, for clarity, we again note that $F_0 := w'_0$.

Bulk term: We consider the individual terms in the summation. Let $B = \sum_{\ell=1}^{\infty} v'_\ell B_\ell$, where we define

$$\begin{aligned}
B_\ell &:= \left\{ \partial_2 V(u'_{\ell-1}, u'_\ell) + \partial_1 V(u'_\ell, u'_{\ell+1}) \right\} - \left\{ \partial_F W(w'_\ell) \right\} \\
&\quad - \left\{ \partial_2 V(F_0 + q'_{\ell-1}, F_0 + q'_\ell) + \partial_1 V(F_0 + q'_\ell, F_0 + q'_{\ell+1}) - \partial_F W(F_0) \right\}.
\end{aligned}$$

For these terms, we include an extra term that is a midpoint approximation for the w' strain in the atomistic force and make use of the identity $\partial_F W(F) = \partial_1 V(F, F) + \partial_2 V(F, F)$ to split B_ℓ into

$$\begin{aligned}
B_\ell &= \left\{ \left[\partial_2 V(u'_{\ell-1}, u'_\ell) + \partial_1 V(u'_\ell, u'_{\ell+1}) \right] - \left[\partial_2 V(w'_\ell + q'_{\ell-1}, w'_\ell + q'_\ell) + \partial_1 V(w'_\ell + q'_\ell, w'_\ell + q'_{\ell+1}) \right] \right\} \\
&\quad + \left\{ \left[\partial_2 V(w'_\ell + q'_{\ell-1}, w'_\ell + q'_\ell) + \partial_1 V(w'_\ell + q'_\ell, w'_\ell + q'_{\ell+1}) \right] - \left[\partial_2 V(w'_\ell, w'_\ell) + \partial_1 V(w'_\ell, w'_\ell) \right] \right\} \\
&\quad - \left\{ \partial_2 V(F_0 + q'_{\ell-1}, F_0 + q'_\ell) + \partial_1 V(F_0 + q'_\ell, F_0 + q'_{\ell+1}) - \partial_2 V(F_0, F_0) - \partial_1 V(F_0, F_0) \right\} \\
&=: B_\ell^{(1)} + B_\ell^{(2)} - B_\ell^{(3)}.
\end{aligned}$$

We first consider $B_\ell^{(1)}$ with a partial midpoint approximation. We can expand the the

site energies and use the definition of $u := w + q$ to find that

$$\begin{aligned}
B_\ell^{(1)} &= \left[\partial_2 V(u'_{\ell-1}, u'_\ell) + \partial_1 V(u'_\ell, u'_{\ell+1}) \right] \\
&\quad - \left[\partial_2 V(w'_\ell + q'_{\ell-1}, w'_\ell + q'_\ell) + \partial_1 V(w_\ell + q'_\ell, w'_\ell + q'_{\ell+1}) \right] \\
&= \partial \partial_2 V(w'_\ell + q'_{\ell-1}, w'_\ell + q'_\ell) \cdot \begin{pmatrix} u'_{\ell-1} - w'_\ell - q'_{\ell-1} \\ u'_\ell - w'_\ell - q'_\ell \end{pmatrix} \\
&\quad + \partial \partial_1 V(w'_\ell + q'_\ell, w'_\ell + q'_{\ell+1}) \cdot \begin{pmatrix} u'_\ell - w'_\ell - q'_\ell \\ u'_{\ell+1} - w'_\ell - q'_{\ell+1} \end{pmatrix} + \mathcal{O}(|w''_{\ell-1}|^2 + |w''_\ell|^2) \\
&= \partial_{12} V(w'_\ell + q'_\ell, w'_\ell + q'_{\ell+1}) \cdot w''_\ell - \partial_{12} V(w'_\ell + q'_{\ell-1}, w'_\ell + q'_\ell) \cdot w''_{\ell-1} \\
&\quad + \mathcal{O}(|w''_{\ell-1}|^2 + |w''_\ell|^2).
\end{aligned}$$

Expanding the result again yields

$$B_\ell^{(1)} = (\partial_{12} V(w'_\ell + q'_\ell, w'_\ell + q'_\ell)) \cdot (w''_\ell - w''_{\ell-1}) + \mathcal{O}(|q''_\ell| \cdot |w''_{\ell-1}| + |q''_\ell| \cdot |w''_\ell| + |w''_{\ell-1}|^2 + |w''_\ell|^2).$$

Thus,

$$|B_\ell^{(1)}| \lesssim |w'''_\ell| + |w''_{\ell-1}|^2 + |w''_\ell|^2 + |q''_\ell| \cdot |w''_{\ell-1}| + |q''_\ell| \cdot |w''_\ell|. \quad (4.11)$$

Finally, we consider the remaining terms in the interior summation. Using the gradient theorem, we may rewrite $B_\ell^{(2)}$ and $B_\ell^{(3)}$ in the following way:

$$\begin{aligned}
B_\ell^{(2)} &= \int_0^1 \partial \partial_2 V(w'_\ell + tq'_{\ell-1}, w'_\ell + tq'_\ell) \cdot \begin{pmatrix} q'_{\ell-1} \\ q'_\ell \end{pmatrix} dt \\
&\quad + \int_0^1 \partial \partial_1 V(w'_\ell + tq'_\ell, w'_\ell + tq'_{\ell+1}) \cdot \begin{pmatrix} q'_\ell \\ q'_{\ell+1} \end{pmatrix} dt, \quad \text{and} \\
B_\ell^{(3)} &= \int_0^1 \partial \partial_2 V(F_0 + tq'_{\ell-1}, F_0 + tq'_\ell) \cdot \begin{pmatrix} q'_{\ell-1} \\ q'_\ell \end{pmatrix} dt \\
&\quad + \int_0^1 \partial \partial_1 V(F_0 + tq'_\ell, F_0 + tq'_{\ell+1}) \cdot \begin{pmatrix} q'_\ell \\ q'_{\ell+1} \end{pmatrix} dt.
\end{aligned}$$

We now consider the difference between $B_\ell^{(2)}$ and $B_\ell^{(3)}$:

$$\begin{aligned} & B_\ell^{(2)} - B_\ell^{(3)} \\ &= \int_0^1 \left(\partial \partial_2 V(w'_\ell + tq'_{\ell-1}, w'_\ell + tq'_\ell) - \partial \partial_2 V(F_0 + tq'_{\ell-1}, F_0 + tq'_\ell) \right) \cdot \begin{pmatrix} q'_{\ell-1} \\ q'_\ell \end{pmatrix} dt \\ &+ \int_0^1 \left(\partial \partial_1 V(w'_\ell + tq'_{\ell-1}, w'_\ell + tq'_\ell) - \partial \partial_1 V(F_0 + tq'_\ell, F_0 + tq'_{\ell+1}) \right) \cdot \begin{pmatrix} q'_\ell \\ q'_{\ell+1} \end{pmatrix} dt. \end{aligned}$$

Taking the absolute value and utilizing the Lipschitz continuity of the Hessians of the site energy, we have that

$$\begin{aligned} |B_\ell^{(2)} - B_\ell^{(3)}| &\lesssim \int_0^1 \begin{pmatrix} |w'_\ell - F_0| \\ |w'_\ell - F_0| \end{pmatrix} \cdot \begin{pmatrix} q'_{\ell-1} \\ q'_\ell \end{pmatrix} dt + \int_0^1 \begin{pmatrix} |w'_\ell - F_0| \\ |w'_\ell - F_0| \end{pmatrix} \cdot \begin{pmatrix} q'_\ell \\ q'_{\ell+1} \end{pmatrix} dt \\ &\lesssim (|q'_{\ell-1}| + |q'_\ell| + |q'_{\ell+1}|) |w'_\ell - F_0|. \end{aligned}$$

Summing this error term along with (4.11) and applying the Cauchy-Schwarz inequality yields the interior contribution of the stated result. \square

Theorem 4.2.3 (Consistency). *Let $\|f\|_{\mathcal{U}^*}$ be sufficiently small and L be sufficiently large so that the conditions of Theorem 2.2.3, Theorem 4.1.1 with $F_0 := \nabla u^{\text{cb}}(0)$, and Proposition 4.1.3 are satisfied. Let u^{cb} and q_L denote the corresponding Cauchy–Born and finite boundary layer corrector solutions. Then,*

$$\|\delta \mathcal{E}^{\text{a}}(\Pi_{\text{a}} u^{\text{cb}} + q_L) - f\|_{\mathcal{U}^*} \lesssim \mu_q^L + |\nabla^2 u^{\text{cb}}(0)| + \|\nabla^2 u^{\text{cb}}\|_{L^4}^2 + \|\nabla^3 u^{\text{cb}}\|_{L^2} + \|\nabla f\|_{L^2}.$$

Proof. Let q_∞ denote the solution to the corrector problem with infinite boundary layer from Theorem 4.1.1. As u^{cb} and q_∞ are solutions to their respective problems, $\langle \delta \mathcal{E}^{\text{cb}}(u^{\text{cb}}), v \rangle = \langle \tilde{g}, \nabla v \rangle_{\mathbb{R}_{\geq 0}}$ for all $v \in \mathcal{U}^{\text{cb}}$ with \tilde{g} defined as in (2.28) and $\langle \delta \mathcal{E}^\Gamma(q_\infty; F_0), v \rangle = 0$ for all $v \in \mathcal{Q}_\infty$. We recall that \mathcal{U} can be seen as a subspace of \mathcal{U}^{cb} and that $\mathcal{Q}_\infty = \mathcal{U}$.

Let $\tilde{u} := \Pi_{\text{a}} u^{\text{cb}} + q_L$ be the predictor-corrector approximation and $F_0 := \nabla u^{\text{cb}}(0)$ as usual. Then, using the fact that u^{cb} solves the Cauchy–Born problem (2.24), we can

split the consistency error into

$$\begin{aligned}
\langle \delta \mathcal{E}^a(\tilde{u}) - f, v \rangle &= \langle \delta_{\text{ext}} + \delta_{\text{cb}} + \delta_{\Gamma} + \delta_{\text{pc}}, v \rangle, \quad \text{where} \\
\delta_{\text{ext}} &:= \langle f, \cdot \rangle_{\mathbb{R}_{\geq 0}} - \langle f, \cdot \rangle_{\mathbb{Z}_{\geq 0}}, \\
\delta_{\text{cb}} &:= \delta \mathcal{E}^{\text{cb}}(\Pi_a u^{\text{cb}}) - \delta \mathcal{E}^{\text{cb}}(u^{\text{cb}}), \\
\delta_{\Gamma} &:= \delta \mathcal{E}^a(\Pi_a u^{\text{cb}} + q_L) - \delta \mathcal{E}^a(\Pi_a u^{\text{cb}} + q_{\infty}), \quad \text{and} \\
\delta_{\text{pc}} &:= \delta \mathcal{E}^a(\Pi_a u^{\text{cb}} + q_{\infty}) - \delta \mathcal{E}^{\text{cb}}(\Pi_a u^{\text{cb}}) - \delta \mathcal{E}^{\Gamma}(q_{\infty}; F_0).
\end{aligned}$$

The term δ_{ext} represents the error in the action of the external forces. In the atomistic model, the external forces can be written as $\langle f, v \rangle_{\mathbb{Z}_{\geq 0}} = \langle g, v' \rangle_{\mathbb{Z}_{\geq 0}}$, where g is defined as in (2.27). Using (2.29), we get that

$$|\langle \delta_{\text{ext}}, v \rangle| = |\langle \tilde{g}, \nabla v \rangle_{\mathbb{R}_{\geq 0}} - \langle g, v' \rangle_{\mathbb{Z}_{\geq 0}}| \lesssim \|\nabla f\|_{L^2} \|v'\|_{\ell^2} \quad \text{for all } v \in \mathcal{U}.$$

The term δ_{cb} represents the error associated with the discretization of the Cauchy–Born problem and was computed in Theorem 2.2.4:

$$\|\delta_{\text{cb}}\|_{\mathcal{U}^*} \lesssim \|\nabla^2 u^{\text{cb}}\|_{L^4}^2.$$

The term δ_{Γ} represents the error associated with the Galerkin projection of the corrector problem and was shown in Theorem 4.1.3 to be

$$\|\delta_{\Gamma}\|_{\mathcal{U}^*} \lesssim \mu_q^L.$$

Finally, for δ_{pc} , the error due to the predictor-corrector method, we use the result from Theorem 4.2.2:

$$\begin{aligned}
\|\delta_{\text{pc}}\|_{\mathcal{U}^*} &\lesssim \|(\Pi_a u^{\text{cb}})''\|_{\ell^4}^2 + \|(\Pi_a u^{\text{cb}})'''\|_{\ell^2} + \|q'' \cdot (\Pi_a u^{\text{cb}})''\|_{\ell^2} \\
&\quad + |(\Pi_a u^{\text{cb}})'_0 - F_0| + \left(\sum_{\ell=1}^{\infty} (|q'_{\ell-1}| + |q'_{\ell}| + |q'_{\ell+1}|)^2 \cdot |(\Pi_a u^{\text{cb}})'_{\ell} - F_0|^2 \right)^{1/2} \\
&=: P_1 + P_2 + P_3 + P_4 + P_5,
\end{aligned}$$

where each P_i is defined as the corresponding term in the previous sum and we have

written $q := q_\infty$ for readability.

To proceed with the computation of the error bound, we need to relate discrete and continuous derivatives for the Cauchy–Born solution. Making use of the definition of the projector Π_a from 2.33

$$\begin{aligned} |(\Pi_a u^{\text{cb}})''_\ell| &= |(\Pi_a u^{\text{cb}})'_{\ell+1} - (\Pi_a u^{\text{cb}})'_\ell| = \left| \int_\ell^{\ell+1} \nabla u^{\text{cb}}(x+1) - \nabla u^{\text{cb}}(x) dx \right| \\ &= \left| \int_\ell^{\ell+1} \int_0^1 \nabla^2 u^{\text{cb}}(x+t) dt dx \right| \leq \int_\ell^{\ell+2} |\nabla^2 u^{\text{cb}}(x)| dx. \end{aligned}$$

Analogously, we can prove that

$$\begin{aligned} |(\Pi_a u^{\text{cb}})'''_\ell| &\leq \int_{\ell-1}^{\ell+2} |\nabla^3 u^{\text{cb}}(x)| dx, \quad \text{and} \\ |(\Pi_a u^{\text{cb}})'_\ell - F_0| &\leq \int_0^{\ell+1} |\nabla^2 u^{\text{cb}}(x)| dx. \end{aligned} \tag{4.12}$$

Using these estimates, it is straightforward to establish that

$$P_1 = \|(\Pi_a u^{\text{cb}})''\|_{\ell^4}^2 \lesssim \|\nabla^2 u^{\text{cb}}\|_{L^4}^2, \quad \text{and} \quad P_2 = \|(\Pi_a u^{\text{cb}})'''\|_{\ell^2} \lesssim \|\nabla^3 u^{\text{cb}}\|_{L^2}.$$

The remaining three terms have a similar structure and will be bound in a like manner. The first cross-term norm will be bounded with an approach similar to the previous norms with the only difference being that we include the exponential bound on the corrector strains of $q \equiv q_\infty$ from Theorem 4.1.1. Due to the exponential bound on q_ℓ , it is easy to show that $|q''_\ell| \lesssim \mu_q^\ell$, where we again note that $0 \leq \mu_q < 1$. There exists an $\alpha > 0$ such that $\mu_q^\ell = e^{-\alpha\ell}$. Now, using the earlier bound on $|(\Pi_a u^{\text{cb}})''_\ell|$, we can show that

$$P_3^2 = \|q'' \cdot (\Pi_a u^{\text{cb}})''\|_{\ell^2}^2 = \sum_{\ell=0}^{\infty} |q''_\ell|^2 \cdot |(\Pi_a u^{\text{cb}})''_\ell|^2 \lesssim \int_0^{\infty} e^{-2\alpha x} |\nabla^2 u^{\text{cb}}(x)|^2 dx.$$

Applying (4.12) and using the fact that $e^{-\alpha x}$ is bounded below on $[0, 1]$, we have that

$$P_4^2 = |(\Pi_a u^{\text{cb}})'_0 - F_0|^2 \lesssim \int_0^1 e^{-2\alpha x} |\nabla^2 u^{\text{cb}}(x)|^2 dx.$$

Finally, applying (4.12) again together with $|q'_\ell| \lesssim \mu_q^\ell = e^{-\alpha\ell}$, we derive the following estimate:

$$\begin{aligned}
P_5^2 &= \sum_{\ell=1}^{\infty} (|q'_{\ell-1}| + |q'_\ell| + |q'_{\ell+1}|)^2 \cdot |(\Pi_a u^{\text{cb}})'_\ell - F_0|^2 \\
&\lesssim \sum_{\ell=1}^{\infty} \mu_q^{2\ell} \left(\int_0^{\ell+1} |\nabla^2 u^{\text{cb}}(x)| dx \right)^2 \lesssim \int_0^\infty e^{-2\alpha t} \left(\int_0^t |\nabla^2 u^{\text{cb}}(x)| dx \right)^2 dt \\
&\lesssim \int_0^\infty e^{-2\alpha t} \int_0^t |\nabla^2 u^{\text{cb}}(x)|^2 dx dt = \int_0^\infty |\nabla^2 u^{\text{cb}}(x)|^2 \int_x^\infty e^{-2\alpha t} dt dx \\
&\lesssim \int_0^\infty (1+x) e^{-2\alpha x} |\nabla^2 u^{\text{cb}}(x)|^2 dx.
\end{aligned}$$

Combining the previous error estimates for the P terms yields

$$P_3^2 + P_4^2 + P_5^2 \lesssim \int_0^\infty (1+x) e^{-2\alpha x} |\nabla^2 u^{\text{cb}}(x)|^2 dx.$$

To finalize, we use the same argument as in the estimate for P_5 to deduce that

$$\begin{aligned}
P_3^2 + P_4^2 + P_5^2 &\lesssim |\nabla^2 u^{\text{cb}}(0)|^2 + \int_0^\infty (1+x) e^{-2\alpha x} |\nabla^2 u^{\text{cb}}(x) - \nabla^2 u^{\text{cb}}(0)|^2 dx \\
&\lesssim |\nabla^2 u^{\text{cb}}(0)|^2 + \int_0^\infty (1+x)^2 e^{-2\alpha x} |\nabla^3 u^{\text{cb}}(x)|^2 dx \\
&\lesssim |\nabla^2 u^{\text{cb}}(0)|^2 + \|\nabla^3 u^{\text{cb}}\|_{L^2}^2.
\end{aligned}$$

Combining the results for $\delta_{\text{ext}}, \delta_{\text{cb}}, \delta_\Gamma$ and those for $P_j, j = 1, \dots, 5$, we arrive at the stated result. \square

Theorem 4.2.4 (Stability). *There exists $\varepsilon, L_0 > 0$ such that for all $f \in \mathcal{U}^*$ with $\|f\|_{\mathcal{U}^*} < \varepsilon$ and all $L \geq L_0$, we have*

$$\langle \delta^2 \mathcal{E}^a(\Pi_a u^{\text{cb}} + q_L)v, v \rangle \geq \frac{c_a}{2} \|v'\|_{\ell^2}^2,$$

where c_a denotes the stability constant for u_{gr}^a .

Proof. First, let f be small enough and L be large enough so that Theorem 2.2.3, Theorem 4.1.1, and Proposition 4.1.3 holds. The second variation of the atomistic

energy evaluated at the predictor-corrector solution can be written as

$$\begin{aligned} \langle \delta^2 \mathcal{E}^a(\Pi_a u^{\text{cb}} + q_L)v, v \rangle &= \langle \delta^2 \mathcal{E}^a(u_{\text{gr}}^a)v, v \rangle - [\langle \delta^2 \mathcal{E}^a(u_{\text{gr}}^a)v, v \rangle - \langle \delta^2 \mathcal{E}^a(q_\infty)v, v \rangle] \\ &\quad - [\langle \delta^2 \mathcal{E}^a(q_\infty)v, v \rangle - \langle \delta^2 \mathcal{E}^a(q_L)v, v \rangle] - [\langle \delta^2 \mathcal{E}^a(q_L)v, v \rangle - \langle \delta^2 \mathcal{E}^a(\Pi_a u^{\text{cb}} + q_L)v, v \rangle]. \end{aligned}$$

The highlighted difference terms can all be bound using the Lipschitz continuity of the second variation of the atomistic energy:

$$|\langle \delta^2 \mathcal{E}^a(u_{\text{gr}}^a)v, v \rangle - \langle \delta^2 \mathcal{E}^a(q_\infty)v, v \rangle| \lesssim \|(u_{\text{gr}}^a)' - (q_\infty)'\|_{\ell^2} \|v'\|_{\ell^2}^2 \quad (4.13)$$

$$|\langle \delta^2 \mathcal{E}^a(q_\infty)v, v \rangle - \langle \delta^2 \mathcal{E}^a(q_L)v, v \rangle| \lesssim \|(q_\infty)' - (q_L)'\|_{\ell^2} \|v'\|_{\ell^2}^2 \quad (4.14)$$

$$|\langle \delta^2 \mathcal{E}^a(q_L)v, v \rangle - \langle \delta^2 \mathcal{E}^a(\Pi_a u^{\text{cb}} + q_L)v, v \rangle| \lesssim \|(\Pi_a u^{\text{cb}})'\|_{\ell^2} \|v'\|_{\ell^2}^2 \quad (4.15)$$

Each of these bounds goes to zero either for large L or for small $\|f\|_{\mathcal{U}^*}$. The bound in (4.13) goes to zero as $\|f\|_{\mathcal{U}^*} \rightarrow 0$ by Theorem 4.1.1, the bound in (4.14) goes to zero as $L \rightarrow \infty$ by Proposition 4.1.3, and the bound in (4.15) goes to zero as $f \rightarrow 0$ by Theorem 2.2.3. Finally, $\langle \delta^2 \mathcal{E}^a(u_{\text{gr}}^a)v, v \rangle \geq c_a \|v'\|_{\ell^2}^2$ by definition. Thus, there exists an $L_0 > 0$ and an $\varepsilon > 0$ such that the theorem statement holds. \square

With the conclusion of the proof of stability, we have proven all of the necessary results for Theorem 4.2.1 to hold. In the next two sections, we discuss the error estimate of the predictor-corrector solution in terms of the applied force and conduct numerical experiments to verify the results of the analysis.

4.2.1 Error Bound in Terms of the External Forces

When discussing the Cauchy–Born model, it is common to consider its convergence to the atomistic model under a standard rescaling of the external force [24, 39]. We wish to examine the predictor-corrector method’s behavior in such a situation. To that end, the error estimate of the previous section can be rewritten using Theorem 2.2.3 in terms of f only:

$$\|(u^a)' - (u_L^{\text{pc}})'\|_{\ell^2} \lesssim \mu_q^L + |f(0)| + \|f\|_{L^4}^2 + \|\nabla f\|_{L^2}. \quad (4.16)$$

We now informally motivate the standard scaling of the external force. Let λ^{-1} denote a length-scale over which we expect elastic strains to vary. After rescaling space

according to $x \rightsquigarrow \lambda x$ and $u \rightsquigarrow \lambda u$, we expect that this variation will now occur on an $O(1)$ scale. The corresponding dual scaling for the external force is $f(x) \rightsquigarrow \lambda f(\lambda x)$. This is the scaling that we will consider in the numerical results section with the external force $f := f^{(\lambda)}$ given by

$$f_\ell^{(\lambda)} := \lambda \hat{f}(\lambda \ell).$$

It is simple to use the prescribed scaling to show that

$$|f^{(\lambda)}(0)| = \lambda |\hat{f}(0)|, \quad \|f^{(\lambda)}\|_{L^4}^2 = \lambda^{3/2} \|\hat{f}\|_{L^4}^2, \quad \text{and} \quad \|\nabla f^{(\lambda)}\|_{L^2} = \lambda^{3/2} \|\nabla \hat{f}\|_{L^2}.$$

As with the atomistic and continuum problems, there exists some $\hat{g} \in H^2$ such that $\hat{f} = -\nabla \hat{g}$. For $\|\hat{g}\|_{H^2}$ sufficiently small, the error bound in Eq. (4.16) holds independent of λ , and we can then show that

$$\|(u^a)' - (u_L^{\text{pc}})'\|_{\ell^2} \lesssim \mu_q^L + \lambda + \lambda^{3/2}.$$

It is clear that the dominant error in this scaling is due to the surface contribution to the error as opposed to the Cauchy–Born modeling error in the interior. We may now balance the error by choosing $L = \log \lambda / \log \mu_q$ to finally obtain

$$\|(u^a)' - (u_L^{\text{pc}})'\|_{\ell^2} \lesssim \lambda + \lambda^{3/2}.$$

We verify the linear dependence on λ for the error in Test 2 in the following section for this scaling of the external force.

Remark. If we take f_λ as a smooth function rather than a piecewise affine interpolant, then the Cauchy–Born solution is rescaled due to the force rescaling according to $\nabla u_\lambda^{\text{cb}}(x) = \nabla u^{\text{cb}}(\lambda x)$. In particular, $\nabla u_\lambda^{\text{cb}}(0)$ would then be independent of λ , and thus the corrector problem is independent of λ as well.

For the choice of interpolation of f used in this analysis, this observation should still be approximately true. Thus, the analysis given for the predictor-corrector method can be made rigorous in the context of the force scaling given in this section.

4.3 Numerical Results

In this section, we provide numerical demonstrations of the predictor-corrector method as well as corroboration of the error estimates we established. We use the EAM model described in 2.1.1.

The semi-infinite chain model as developed above contains an infinite number of degrees of freedom and cannot be minimized numerically. Therefore, we will instead consider an approximation of the semi-infinite chain model that has only a finite number of strain degrees of freedom with the rest fixed. We will seek energy-minimizing configurations in the space

$$\mathcal{U}_N := \{u \in \mathcal{U} \mid u'_\ell = 0 \text{ for } \ell \geq N\}.$$

The existence of a solution to the atomistic system in such a space for large enough N is an easy consequence of the quantitative inverse function theorem. The difference between the approximate solution in this space and the actual solution is dependent on the rate of decay of the atomistic solution. From theorem 2.1.2, the decay was shown to be exponential in the strongly stable ground state. Provided that N is sufficiently large in comparison to the support of f , it can trivially be proven using the techniques employed thus far in the analysis that the additional error committed is exponentially small in N . As a result of this exponentially decreasing error, it is realistically possible to choose a large enough N such that the difference between the approximate solution and the actual solution is quite small. Due to the low computational cost in one-dimensional experiments, we choose $N = 1000$ throughout in order to guarantee that the additional error committed from replacing \mathcal{U} with \mathcal{U}_N is negligible.

We will need to consider an approximation of the Cauchy–Born model as well; however, here, we can simply seek minimizers of a discretized Cauchy–Born model:

$$\mathcal{E}^{\text{cb}}(u) := \sum_{\ell=0}^{\infty} W(u'_\ell), \quad \text{where} \quad W(F) = \frac{1}{2}\phi(1+F) + \frac{1}{2}\phi(1+F) + \psi(2\rho(1+F)).$$

Proposition 2.2.4 can be employed to prove that this discretization does not introduce new terms to the error bound (4.9). Due to the local nature of the Cauchy–Born model, we can still look for minimizers in an infinite dimensional space provided that

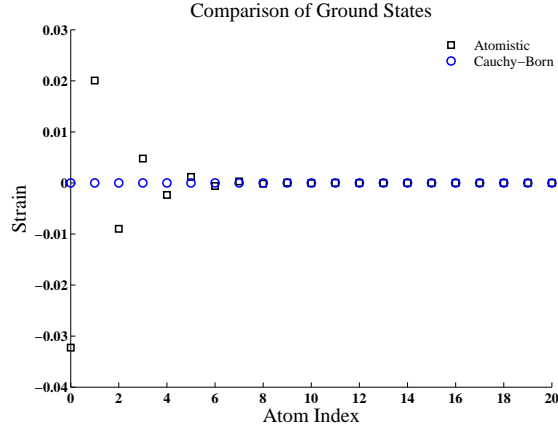


Figure 4.1: Ground states for the atomistic and Cauchy–Born models.

the external force f is only non-zero for a finite number of elements. Wherever it is zero, the minimizing strain value will simply be 0 due to how we constructed the model. The corrector method needs no further modification since we always consider finite boundary layers.

The energy-minimizing configurations for the above models are found using the steepest-descent method with a backtracking algorithm.

Test 1: Ground State

In the first numerical ground state, we compute the ground states ($f = 0$) of the atomistic, pure Cauchy–Born, and predictor-corrector method which are shown in Figures 4.1 and 4.2. The atomistic ground state exhibits the predicted exponential decay. In addition to this behavior, we also observe an alternating sign in the strain, a behavior that the EAM model under consideration is intended to capture.

The pure Cauchy–Born solution clearly does not capture any surface effects: its solution is the zero strain as mentioned earlier. For the predictor-corrector method solutions, we see that u_2^{PC} is already a good approximation while u_5^{PC} is almost visually indistinguishable from u_{gr}^{a} over its boundary layer.

Since $f = 0$ and the Cauchy–Born solution is $\nabla u^{\text{cb}} = 0$, it is easy to see that the Cauchy–Born error contributions and the error in the approximation of the external force for the predictor-corrector method error bound in 4.9 vanish. The only remaining error

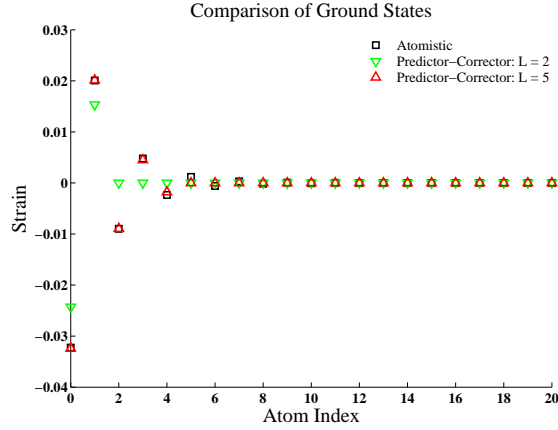


Figure 4.2: Ground states for the atomistic model and the predictor-corrector method.

is the corrector’s finite boundary layer error contribution. We numerically demonstrate the exponential convergence of $q_L = u_L^{\text{PC}}$ to the atomistic ground state in Figure 4.3.

Test 2: Long Wavelength Limit

We next consider the behavior of the error in the predictor-corrector method’s approximation of the atomistic ground state under the usual long-wavelength limit described in § 4.2.1. For this test, we define $\hat{f}(x) := \cos(3\pi x/8)\chi_{[0,4)}(x)$, where $\chi_A(x)$ denotes the characteristic function, and let the applied force be given by $f_\ell := \lambda \hat{f}(\lambda \ell)$. The choice of the size of the boundary layer, L , is motivated from a balancing of the error terms in the predictor-corrector method approximation as mentioned in the remarks after Theorem 4.2.1. For each λ , we compute the solution to the predictor-corrector method with the size of the boundary layer set to be $L = 3 + \lceil \log_{10/9}(\lambda^{-1}) \rceil$. The base of the logarithm was selected to be less than μ_q^{-1} , the base in the exponential decay of the corrector solution. This ensures that the surface contribution to the error becomes λ^η where $\eta > 1$ is a constant. The value of μ_q was numerically estimated in order to choose the value of 10/9 as the logarithm’s base. Figure 4.4 shows the first-order convergence that results when the scaling factor λ is taken to zero. The predictor-corrector method behaves precisely as predicted in § 4.2.1.

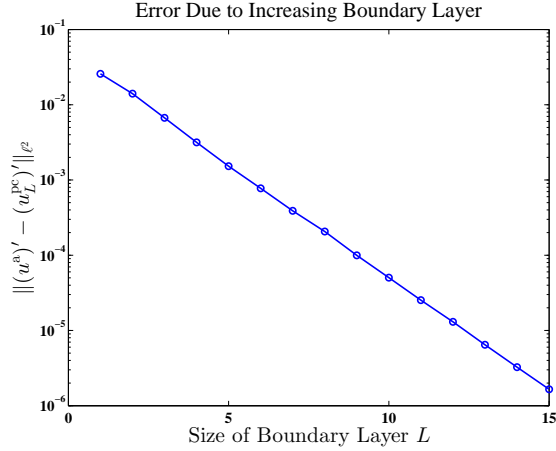


Figure 4.3: Rate of convergence to atomistic solution in infinite boundary layer limit.

Test 3: Error with External Forces

We conclude the numerical experiments by highlighting the fact that the error made by the predictor-corrector method’s approximation will not vanish with increasing boundary layer in the case of fixed non-zero external forces. To that end, we consider $f_\ell = \hat{f}(\ell)$, where \hat{f} is as in the previous test. In Figure 4.5, we display the energy-minimizing configurations for the atomistic solution, the Cauchy–Born solution, and the predictor-corrector method with $L = 5$. We note that the Cauchy–Born solution is no longer trivial and that the predictor-corrector approximation is not quite as accurate as in the case of zero external forces. In Figure, 4.6, we numerically demonstrate that the error in the predictor-corrector’s method approximation does not vanish as the boundary layer is taken increasingly large. We observe that a small error in the boundary layer still persists. Indeed, since the error depends on the magnitude and regularity of f as demonstrated in Eq. (4.16), it cannot be driven to zero. We emphasize, however, that despite our extremely concentrated and non-smooth choice of f , the predictor-corrector method is able to reduce the error by a factor of 30, which is an excellent improvement given the simplicity of the chosen predictor-corrector scheme.

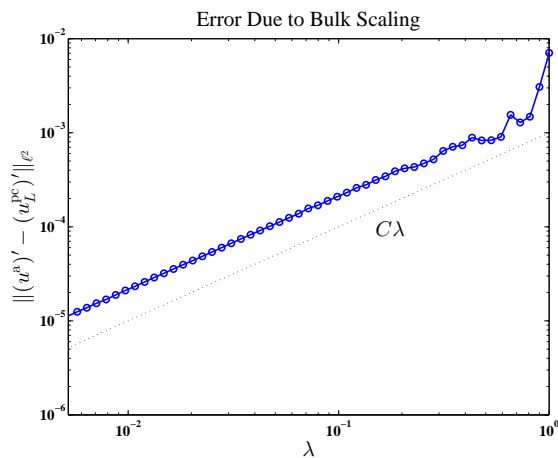


Figure 4.4: Rate of convergence to atomistic solution in the long-wavelength limit.

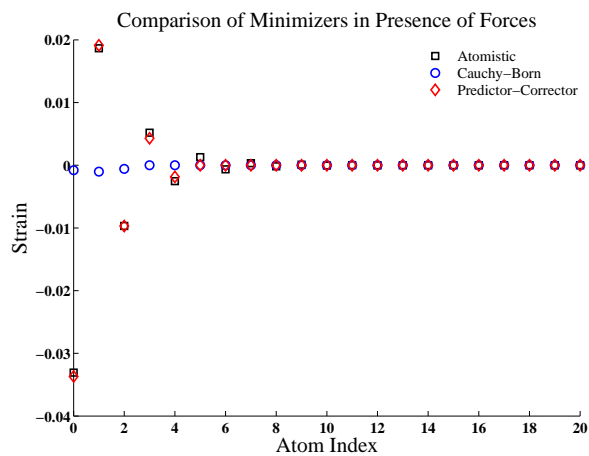


Figure 4.5: Energy-minimizing configuration for atomistic and predictor-corrector systems in the presence of external forces ($L = 5$).

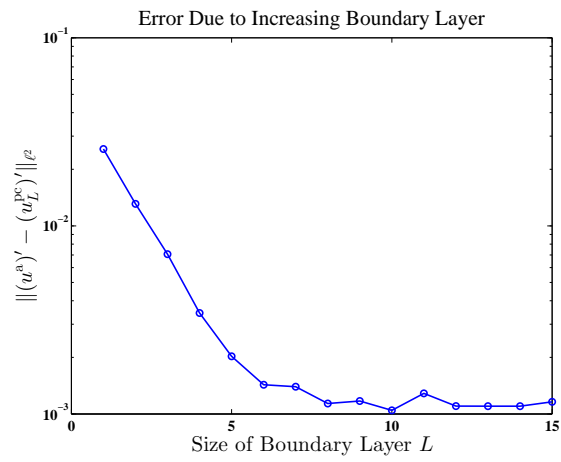


Figure 4.6: Demonstration of non-vanishing error in the presence of non-zero external forces and increasing boundary layer.

Chapter 5

Conclusion

In this work, a detailed analysis of a 1D surface model problem was produced. We proved the existence of ground states exhibiting surface effects for the atomistic model. In addition, it was shown that these surface effects are extremely concentrated at the surface. The regular Cauchy-Born method, often used to model bulk materials, was shown to be inadequate for the task of capturing these surface effects. To address this issue, two different approaches were considered.

In the surface Cauchy-Born method, a surface energy integral was introduced in order to capture missed surface effects. The addition of this surface integral restored the agreement with the atomistic model for homogeneous strains that was lost in the regular Cauchy-Born method. The analysis showed that the surface Cauchy-Born method does indeed represent an improvement over the regular Cauchy-Born method in a given physical parameter regime. However, the method lacks a systematic form of control over the error. In addition, even for materials which lie in the appropriate parameter regime, the surface Cauchy-Born method cannot entirely account for surface relaxation. This prompted consideration of another method.

Since surface effects had been shown to be extremely concentrated at the surface, a new method was suggested in which the regular Cauchy-Born solution, which nicely captures the bulk material behavior, would be post-processed in order to capture the missed surface effects. By solving a computationally cheap surface cell-problem, a corrector strain was produced to form a predictor-corrector approximation of the atomistic solution. A sharp error analysis of this predictor-corrector method was given, and the

convergence of this approximation to the atomistic solution in natural limits was proven. Numerical results show promising quantitative behavior of the proposed scheme.

Despite the analysis of these two methods being one-dimensional, it is anticipated that they can shed some light in higher-dimensional cases when surface behavior dominates edge or corner effects. An important new effect that will have to be taken into account in higher dimensions are surface stresses that act tangentially. Despite the presence of this additional stress, we still expect surface effects to be quite localized for certain higher-dimensional systems as numerical experiments in [38] and analysis in [45] have indicated exponentially decaying responses in 2D; thus, we are optimistic regarding the validity of an extension of the proposed approaches in this work to higher dimensions.

References

- [1] A. Binder, M. Luskin, D. Perez, and A. F. Voter. Analysis of transition state theory rates upon spatial coarse-graining. *Multiscale Modeling & Simulation*, 13(3):890–915, 2015, <http://dx.doi.org/10.1137/140983963>.
- [2] A. Binder, T. Lelièvre, and G. Simpson. A generalized parallel replica dynamics. *Journal of Computational Physics*, 284:595–616, 2015.
- [3] A. J. Binder, M. Luskin, and C. Ortner. Analysis of a predictor-corrector method for computationally efficient modeling of surface effects in 1d. *ArXiv e-prints*, 1605.05750, 2016.
- [4] R.C. Cammarata. Surface and interface stress effects on interfacial and nanostructured materials. *Mat. Sci. Eng. A*, 237(2):180 – 184, 1997.
- [5] R. C. Cammarata and K. Sieradzki. Effects of surface stress on the elastic moduli of thin films and superlattices. *Phys. Rev. Lett.*, 62:2005–2008, Apr 1989.
- [6] S. Cuenot, C. Frétiigny, S. Demoustier-Champagne, and B. Nysten. Surface tension effect on the mechanical properties of nanomaterials measured by atomic force microscopy. *Phys. Rev. B*, 69:165410, Apr 2004.
- [7] J. Diao, K. Gall, and M. L. Dunn. Surface-stress-induced phase transformation in metal nanowires. *Nature Materials*, 2(10):656–660, 2003.
- [8] H. S. Park, K. Gall, and J. A. Zimmerman. Shape memory and pseudoelasticity in metal nanowires. *Phys. Rev. Lett.*, 95:255504, Dec 2005.

- [9] K. Gall, J. Diao, and M. L. Dunn. The strength of gold nanowires. *Nano Letters*, 4(12):2431–2436, 2004, <http://dx.doi.org/10.1021/nl048456s>.
- [10] J. Knap and M. Ortiz. Effect of indenter-radius size on au(001) nanoindentation. *Phys. Rev. Lett.*, 90:226102, Jun 2003.
- [11] R.E. Miller and D. Rodney. On the nonlocal nature of dislocation nucleation during nanoindentation. *Journal of the Mechanics and Physics of Solids*, 56(4):1203 – 1223, 2008.
- [12] E. B. Tadmor and R. E. Miller. *Modeling Materials: Continuum, Atomistic, and Multiscale Techniques*. Cambridge University Press, 2011.
- [13] X. Blanc, C. Le Bris, and P.-L. Lions. From molecular models to continuum mechanics. *Arch. Rat. Mech. Anal.*, 164(4):341–381, 2002.
- [14] A. Braides and M. Cicalese. Surface energies in nonconvex discrete systems. *Math. Models Methods Appl. Sci.*
- [15] R. Alicandro and M. Cicalese. A general integral representation result for continuum limits of discrete energies with superlinear growth. *SIAM J. Math. Anal.*, 36(1):1–37, 2004, <http://dx.doi.org/10.1137/S0036141003426471>.
- [16] E. Weinan and P. Ming. Cauchy–born rule and the stability of crystalline solids: static problems. *Arch. Rat. Mech. Anal.*, 183(2):241–297, 2007.
- [17] H. S. Park, P. A. Klein, and G. J. Wagner. A surface Cauchy-Born model for nanoscale materials. *International Journal for Numerical Methods in Engineering*, 68(10):1072–1095, 2006.
- [18] Harold S. Park. A multiscale finite element method for the dynamic analysis of surface-dominated nanomaterials. *International Journal for Numerical Methods in Engineering*, 83(8-9):1237–1254, 2010.
- [19] H. S. Park and P. A. Klein. A surface Cauchy-Born model for silicon nanostructures. *Comp. Meth. Appl. Mech. Eng.*, 197(41-42):3249 – 3260, 2008. Recent Advances in Computational Study of Nanostructures.

- [20] E. B. Tadmor, M. Ortiz, and R. Phillips. Quasicontinuum analysis of defects in solids. *Philos. Mag. A*, 73:1529–1563, 1996.
- [21] C. Ortner and E. Süli. Analysis of a quasicontinuum method in one dimension. *M2AN Math. Model. Numer. Anal.*, 42(1):57–91, 2008.
- [22] C. Ortner. A priori and a posteriori analysis of the quasinonlocal quasicontinuum method in 1D. *Math. Comp.*, 80(275):1265–1285, 2011.
- [23] M. Dobson, M. Luskin, and C. Ortner. Accuracy of quasicontinuum approximations near instabilities. *J. Mech. Phys. Solids*, 58(10):1741–1757, 2010.
- [24] M. Luskin and C. Ortner. Atomistic-to-continuum coupling. *Acta Numerica*, 22:397–508, 2013.
- [25] M. Dobson and M. Luskin. An analysis of the effect of ghost force oscillation on quasicontinuum error. *ESAIM: M2AN*, 43(3):591–604, 2009.
- [26] P. Ming and J. Yang. Analysis of a one-dimensional nonlocal quasi-continuum method. *Multiscale Modeling & Simulation*, 7:1838–1875, 2009.
- [27] M. Dobson, M. Luskin, and C. Ortner. Sharp stability estimates for the force-based quasicontinuum approximation of homogeneous tensile deformation. *Multiscale Model. Simul.*, 8(3):782–802, 2010.
- [28] M. Dobson, M. Luskin, and C. Ortner. Stability, instability, and error of the force-based quasicontinuum approximation. *Arch. Ration. Mech. Anal.*, 197(1):179–202, 2010.
- [29] D. Olson and C. Ortner. Regularity and locality of point defects in multilattices. *ArXiv e-prints*, 1608.08930, 2016.
- [30] X. H. Li, C. Ortner, A. Shapeev, and B. Van Koten. Analysis of blended atomistic/continuum hybrid methods. *Numer. Math.*, 134, 2016. to appear in Numer. Math.
- [31] M. Luskin, C. Ortner, and B. Van Koten. Formulation and optimization of the energy-based blended quasicontinuum method. *Comput. Methods Appl. Mech. Engrg.*, 253, 2013.

- [32] Derek Olson. *Formulation and Analysis of an Optimization-Based Atomistic-to-Continuum Coupling Algorithm*. PhD thesis, University of Minnesota, 9 2015.
- [33] Gao Wei, Yu Shouwen, and Huang Ganyun. Finite element characterization of the size-dependent mechanical behaviour in nanosystems. *Nanotechnology*, 17:1118, 2006.
- [34] M. E. Gurtin and A. I. Murdoch. A continuum theory of elastic material surfaces. *Arch. Rat. Mech. Anal.*, 57(4):291–323, 1975.
- [35] R. E. Miller and V. B. Shenoy. Size-dependent elastic properties of nanosized structural elements. *Nanotechnology*, 11(3):139, 2000.
- [36] A. Javili and P. Steinmann. A finite element framework for continua with boundary energies. part i: The two-dimensional case. *Computer Methods in Applied Mechanics and Engineering*, 198(27):2198–2208, 2009.
- [37] H. S. Park and P. A. Klein. Surface Cauchy-Born analysis of surface stress effects on metallic nanowires. *Phys. Rev. B*, 75:085408, Feb 2007.
- [38] K. Jayawardana, C. Mordacq, C. Ortner, and H. S. Park. An analysis of the boundary layer in the 1D surface Cauchy-Born Model. *ESAIM: Math. Model. Numer. Anal.*, 47, 2013.
- [39] C. Ortner and F. Theil. Justification of the Cauchy-Born approximation of elastodynamics. *Arch. Ration. Mech. Anal.*, 207, 2013.
- [40] G. B. Folland. *Real Analysis: Modern Techniques and Their Applications (2nd Ed)*. Wiley-Intersciences, 1999.
- [41] R. A. Johnson. Analytic nearest-neighbor model for fcc metals. *Phys. Rev. B*, 37:3924–3931, Mar 1988.
- [42] M. S. Daw and M. I. Baskes. Embedded-atom method: Derivation and application to impurities, surfaces, and other defects in metals. *Phys. Rev. B*, 29:6443–6453, Jun 1984.

- [43] J. E. Jones. On the Determination of Molecular Fields. II. From the Equation of State of a Gas. *Proceedings of the Royal Society of London A: Mathematical, Physical and Engineering Sciences*, 106(738):463–477, 1924.
- [44] J E Lennard-Jones. Cohesion. *Proceedings of the Physical Society*, 43(5):461, 1931.
- [45] F. Theil. Surface energies in a two-dimensional mass-spring model for crystals. *ESAIM: Mathematical Modelling and Numerical Analysis*, 45:873–899, 2011.

Appendix A

Common Results

A.1 Variations in Energies

Proposition A.1.1 (First Variations.). *Let $u, v \in \mathcal{U}$. Then,*

$$\begin{aligned} \langle \delta \mathcal{E}^a(u), v \rangle &= v'_0 \left\{ \partial_1 V^{\text{surf}}(u'_0) + \partial_1 V(u'_0, u'_1) \right\} \\ &\quad + \sum_{\ell=1}^{\infty} v'_\ell \left\{ \partial_2 V(u'_{\ell-1}, u'_\ell) + \partial_1 V(u'_\ell, u'_{\ell+1}) \right\}, \\ \langle \delta \mathcal{E}^\Gamma(q; u^{\text{cb}}), v \rangle &= v'_0 \left\{ \partial_1 V^{\text{surf}}(F_0 + q'_0) + \partial_1 V(F_0 + q'_0, F_0 + q'_1) - \partial_F W(F_0) \right\}, \\ &\quad + \sum_{\ell=1}^{\infty} v'_\ell \left\{ \partial_2 V(F_0 + q'_{\ell-1}, F_0 + q'_\ell) + \partial_1 V(F_0 + q'_\ell, F_0 + q'_{\ell+1}) - \partial_F W(F_0) \right\}. \end{aligned}$$

Let $u, v \in \mathcal{U}^{\text{cb}}$. Then,

$$\langle \delta \mathcal{E}^{\text{cb}}(u), v \rangle = \int_0^\infty \partial_F W(\nabla u) \cdot \nabla v dx \tag{A.1}$$

Proposition A.1.2 (Second Variations.). *Let $u, v, w \in \mathcal{U}$. Then,*

$$\begin{aligned}
\langle \delta^2 \mathcal{E}^a(u)w, v \rangle &= v'_0 F_0 \left\{ \partial_F^2 V^{\text{surf}}(u'_0) + \partial_{11}^2 V(u'_0, u'_1) \right\} + v'_0 w'_1 \left\{ \partial_{12}^2 V(u'_0, u'_1) \right\} \\
&+ \sum_{\ell=1}^{\infty} v'_\ell \left[w'_{\ell-1} \left\{ \partial_{12}^2 V(u'_{\ell-1}, u'_\ell) \right\} + w'_\ell \left\{ \partial_{22}^2 V(u'_{\ell-1}, u'_\ell) + \partial_{11}^2 V(u'_\ell, u'_{\ell+1}) \right\} \right. \\
&\quad \left. + w'_{\ell+1} \left\{ \partial_{12}^2 V(u'_\ell, u'_{\ell+1}) \right\} \right] \\
\langle \delta^2 \mathcal{E}^\Gamma(q; u^{\text{cb}})w, v \rangle &= v'_0 F_0 \left\{ \partial_F^2 V^{\text{surf}}(F_0 + q'_0) + \partial_{11}^2 V(F_0 + q'_0, F_0 + q'_1) \right\} \\
&+ v'_0 w'_1 \left\{ \partial_{12}^2 V(F_0 + q'_0, F_0 + q'_1) \right\} \\
&+ \sum_{\ell=1}^{\infty} v'_\ell \left[w'_{\ell-1} \left\{ \partial_{12}^2 V(F_0 + q'_{\ell-1}, F_0 + q'_\ell) \right\} \right. \\
&\quad \left. + w'_\ell \left\{ \partial_{22}^2 V(F_0 + q'_{\ell-1}, F_0 + q'_\ell) + \partial_{11}^2 V(F_0 + q'_\ell, F_0 + q'_{\ell+1}) \right\} \right. \\
&\quad \left. + w'_{\ell+1} \left\{ \partial_{12}^2 V(F_0 + q'_\ell, F_0 + q'_{\ell+1}) \right\} \right]
\end{aligned}$$

Let $u, v, w \in \mathcal{U}^{\text{cb}}$. Then,

$$\langle \delta^2 \mathcal{E}^{\text{cb}}(u)w, v \rangle = \int_0^\infty \partial_F^2 W(\nabla u) \cdot \nabla w \cdot \nabla v dx \tag{A.2}$$

A.2 Inverse Function Theorem

Theorem A.2.1. *Let \mathcal{H} be a Hilbert space equipped with norm $\|\cdot\|_{\mathcal{H}}$, and let $\mathcal{G} \in C^1(\mathcal{H}, \mathcal{H}^*)$ with Lipschitz-continuous derivative $\delta\mathcal{G}$:*

$$\|\delta\mathcal{G}(u) - \delta\mathcal{G}(v)\|_{\mathcal{L}} \leq M \|u - v\|_{\mathcal{H}} \quad \text{for all } u, v \in \mathcal{H}, \tag{A.3}$$

where $\|\cdot\|_{\mathcal{L}}$ denotes the $\mathcal{L}(\mathcal{H}, \mathcal{H}^*)$ -operator norm.

Let $\bar{u} \in \mathcal{H}$ satisfy

$$\begin{aligned}
\|\mathcal{G}(\bar{u})\|_{\mathcal{H}^*} &\leq \eta \\
\langle \delta\mathcal{G}(\bar{u})v, v \rangle &\geq \gamma \|v\|_{\mathcal{H}}^2 \quad \text{for all } v \in \mathcal{H},
\end{aligned}$$

such that M, η, γ satisfy the relation

$$\frac{2M\eta}{\gamma^2} < 1. \quad (\text{A.4})$$

Then, there exists a (locally unique) $u \in \mathcal{H}$ such that $\mathcal{G}(u) = 0$,

$$\|u - \bar{u}\|_{\mathcal{H}} \leq 2\frac{\eta}{\gamma}, \quad \text{and}$$

$$\langle \delta\mathcal{G}(u)v, v \rangle \geq \left(1 - \frac{2M\eta}{\gamma^2}\right) \gamma \|v\|_{\mathcal{H}}^2 \quad \text{for all } v \in \mathcal{H}.$$

Proof. See [21].

□